Developmental Cell
Article

Establishment of Centromeric Chromatin by the CENP-A Assembly Factor CAL1 Requires FACT-Mediated Transcription

Chin-Chi Chen,[1] Sarion Bowers,[1,5] Zoltan Lipinszki,[2,3] Jason Palladino,[1] Sarah Trusiak,[1] Emily Bettini,[1] Leah Rosin,[1] Marcin R. Przewloka,[2] David M. Glover,[2] Rachel J. O'Neill,[1,4] and Barbara G. Mellone[1,4,*]
[1]Department of Molecular and Cell Biology, University of Connecticut, Storrs, CT 06269, USA
[2]Department of Genetics, University of Cambridge, Cambridge CB2 3EH, UK
[3]Biological Research Centre of the Hungarian Academy of Sciences, Institute of Biochemistry, P.O. Box 521, 6701 Szeged, Hungary
[4]Institute for Systems Genomics, University of Connecticut, Storrs, CT 06269, USA
[5]Present address: Wellcome Trust Sanger Institute, Cambridge CB10 1SA, UK
*Correspondence: barbara.mellone@uconn.edu
http://dx.doi.org/10.1016/j.devcel.2015.05.012

SUMMARY

Centromeres are essential chromosomal structures that mediate accurate chromosome segregation during cell division. Centromeres are specified epigenetically by the heritable incorporation of the centromeric histone H3 variant CENP-A. While many of the primary factors that mediate centromeric deposition of CENP-A are known, the chromatin and DNA requirements of this process have remained elusive. Here, we uncover a role for transcription in *Drosophila* CENP-A deposition. Using an inducible ectopic centromere system that uncouples CENP-A deposition from endogenous centromere function and cell-cycle progression, we demonstrate that CENP-A assembly by its loading factor, CAL1, requires RNAPII-mediated transcription of the underlying DNA. This transcription depends on the CAL1 binding partner FACT, but not on CENP-A incorporation. Our work establishes RNAPII passage as a key step in chaperone-mediated CENP-A chromatin establishment and propagation.

INTRODUCTION

Accurate chromosome segregation during cell division is dependent on the correct assembly and propagation of a distinct region of the chromosome known as the centromere. The centromere forms the structural basis for the assembly of the kinetochore, a multi-protein complex to which spindle microtubules attach during mitosis and meiosis. In most eukaryotes, the position of the centromere is defined epigenetically through the heritable incorporation of the histone H3 variant CENP-A, which is both necessary and sufficient for centromere activity (De Rop et al., 2012).

Centromeric chromatin displays a conserved organization composed of interspersed blocks of CENP-A and H3 nucleosomes (Blower et al., 2002). During DNA replication in human cells, no new CENP-A deposition occurs (Jansen et al., 2007), and histone H3.3 and H3.1 are deposited as placeholders (Dunleavy et al., 2011). CENP-A deposition occurs during or after mitosis in *Drosophila* and humans, respectively (Hemmerich et al., 2008; Jansen et al., 2007; Mellone et al., 2011; Schuh et al., 2007) and is mediated by specialized histone chaperones known as Scm3 in fungi (Camahort et al., 2007; Pidoux et al., 2009; Stoler et al., 2007), HJURP in tetrapods (Barnhart et al., 2011; Bernad et al., 2011; Dunleavy et al., 2009; Foltz et al., 2009; Sanchez-Pulido et al., 2009; Shuaib et al., 2010), and CAL1 in flies (Chen et al., 2014). Each of these chaperones has been shown to selectively bind CENP-A, and not canonical H3, and to mediate the formation of CENP-A nucleosomes in vitro. However, how placeholder nucleosomes are reorganized to incorporate CENP-A/H4 tetramers is unknown. Additional histone chaperones have been found to either bind to CENP-A or contribute to proper CENP-A localization in vertebrate cells (Foltz et al., 2006; Okada et al., 2009; Perpelescu et al., 2009), but whether or not they are involved in this reorganization is unknown.

Mounting evidence points to a functional interplay between the transcription of centromeric repeats and centromere function across species. For instance, manipulation of a human artificial chromosome (HAC) revealed that targeting a transcriptional silencer to alpha-satellite repeats caused loss of CENP-A (Nakano et al., 2008). Remarkably, transcripts emanating from centromeric DNA have been identified in yeast, human, wallabies, and plants (Carone et al., 2009; Chan et al., 2012; Choi et al., 2011; Ohkuni and Kitagawa, 2011; Quénet and Dalal, 2014; Topp et al., 2004) and have been shown to be important for centromere integrity. However, the idea that specific RNAs play a role in centromere integrity is inconsistent with the notion that centromeres can form independently of centromeric DNA (Marshall et al., 2008). Additionally, the functional significance of transcription in the CENP-A assembly cascade remains poorly defined.

Here, we identify RNA polymerase II (RNAPII)-dependent transcription as a key requirement for *Drosophila* CENP-A deposition. Using an inducible ectopic centromere system, which allows for the direct comparison of chromatin states in the

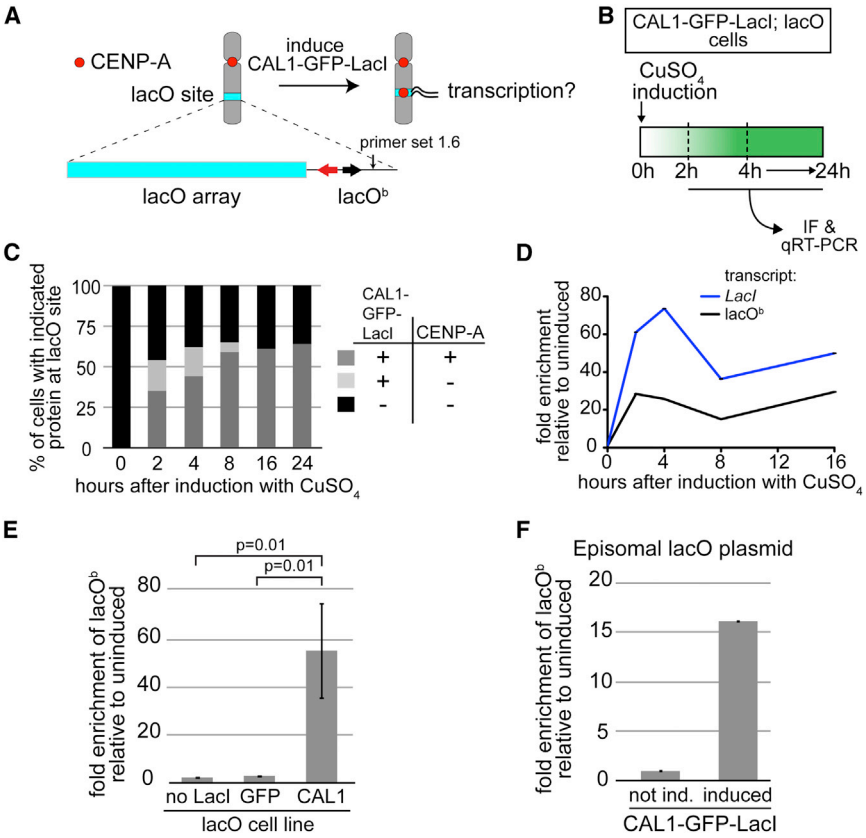

Figure 1. CENP-A Deposition at the Ectopic lacO Site Is Associated with Transcription

(A) Experimental approach to determine if transcription is coupled with CENP-A deposition. The lacO vector is stably inserted in S2 cells and contains 256 lacO repeats (lacO array; blue bar), the bacterial Amp resistance gene (black arrow), and the yeast TRP1 gene (red arrow). Primer set 1.6 (arrow) is within the lacO vector backbone ($lacO^b$).

(B) Experimental strategy used to follow ectopic CENP-A deposition and transcription from $lacO^b$ after induction of CAL1-GFP-LacI.

(C) Quantification of the presence (+) or absence (–) of CAL1-GFP-LacI and CENP-A foci at the lacO site during a time course. n = 100 cells for each time point.

(D) qRT-PCR analysis of $lacO^b$ (black) and CAL1-GFP-LacI transcripts (blue) in induced CAL1-GFP-LacI cells at the indicated times. Error bars, SD of three technical replicates.

(E) qRT-PCR measuring $lacO^b$ transcription after 24 hr induction in cell lines: lacO only (no LacI), lacO with GFP-LacI (GFP), and lacO with CAL1-GFP-LacI (CAL1). The means ± SD of three experiments are shown. p = 0.01, unpaired t test.

(F) Transcription from $lacO^b$ determined by qRT-PCR in CAL1-GFP-LacI cells (induced 24 hr), where the lacO plasmid is episomal. Error bars, 95% confidence interval (CI) of three technical replicates.

See also Figure S1.

presence or absence of active CENP-A deposition, we find that CENP-A assembly by its loading factor CAL1 is coupled with transcription of the underlying DNA. We identify facilitates chromatin transcription (FACT; Orphanides et al., 1998) as a central molecular player in this process and show that its role in centromere integrity is that of driving DNA sequence-independent RNAPII transcription through centromeric chromatin via a direct interaction with CAL1. Thus, current models for centromere transcription must take into account the transcriptional requirements for CENP-A recruitment by its assembly factor.

RESULTS

De Novo CENP-A Incorporation Temporally Coincides with Transcription of the Underlying DNA

Transcription of centromeric DNA has been described in several species (Chan and Wong, 2012), but whether or not it is directly linked to CENP-A deposition has remained elusive. One limitation of studying transcription at endogenous centromeres is the inability to precisely compare the same genomic locus in the presence and absence of active CENP-A deposition without interfering with cell-cycle progression or global transcription, which can result in reciprocal perturbation (Adolph et al., 1993; Whitfield et al., 2002). Furthermore, the endogenous CENP-A-bound DNA sequences of *Drosophila* are unknown, making an assessment of their transcription unfeasible. To overcome these limitations, we employed an ectopic centromere strategy based on the LacI/lacO system (Straight et al., 1996). This system utilizes a stably inserted lacO vector (10 kb of lacO repeats and 3 kb of vector backbone inserted within one arm of chromosome 2 or 3; Mendiburo et al., 2011), coupled with the inducible expression of the *Drosophila* CENP-A chaperone CAL1 fused to the lac repressor LacI (CAL1-GFP-LacI; Figure 1A). A GFP-LacI protein is used as a negative control. lacO-tethered CAL1-GFP-LacI induces the formation of fully functional and epigenetically propagated ectopic centromeres at the lacO site (Chen et al., 2014), allowing the direct comparison of the transcriptional status between lacO DNA with or without ongoing CENP-A incorporation.

CAL1-GFP-LacI is under the control of a metallothionein (MT) promoter, which can be induced by addition of $CuSO_4$ to the growth medium. First, we investigated how long after induction of CAL1-GFP-LacI CENP-A foci become visible at the lacO site by immunofluorescence (IF) on metaphase chromosome spreads. In parallel, we assessed transcription from the lacO backbone ($lacO^b$) by qRT-PCR (primer set 1.6; Figures 1A and 1B; Mendiburo et al., 2011). Transcription of the lacO array portion of the vector could not be assessed by this method due to its repetitive nature. 2 hr after induction, 54% of metaphase spreads displayed CAL1-GFP-LacI foci on the lacO-containing chromosome arm, with ~65% of these foci also containing CENP-A, showing that the recruitment of CENP-A at the lacO site occurs soon after CAL1-GFP-LacI induction (Figure 1C). Strikingly, at the 2 hr time point, a 28-fold change in transcription from $lacO^b$ was detected by qRT-PCR. Furthermore, $lacO^b$ transcript abundance persisted throughout the remainder of the time course (Figure 1D). *LacI* and $lacO^b$

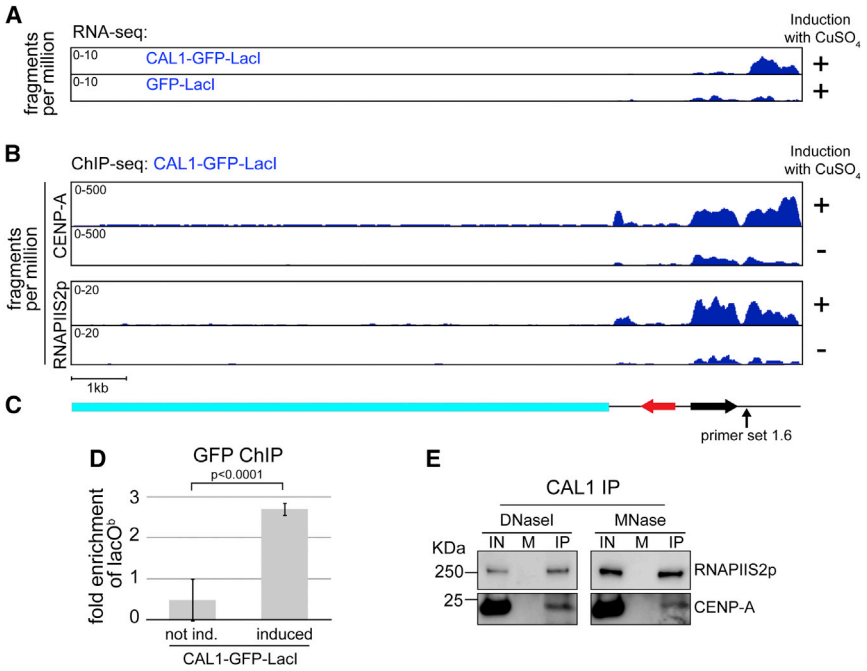

Figure 2. Transcription of lacO^b Correlates with CENP-A and RNAPII Distribution

(A) Coverage tracks of paired-end RNA-seq from induced (24 hr) CAL1-GFP-LacI (top) and GFP-LacI cells (bottom), mapped to the lacO vector. The x axis represents the position along the vector, and the y axis represents the fragments per million reads (normalized to the sequencing depth of each library). $p < 0.05$ (see the Supplemental Experimental Procedures).

(B) Coverage tracks of CENP-A and RNAPIIS2p paired-end ChIP-seq from induced (24 hr) and uninduced CAL1-GFP-LacI cells, mapped to the lacO vector. The x axis represents the position along the vector, and the y axis represents the fragments per million reads (normalized to the sequencing depth of each library).

(C) Schematic of the lacO vector as in Figure 1A.

(D) GFP ChIP-qPCR in CAL1-GFP-LacI uninduced and induced cells (24 hr). Error bars, 95% CI. p value, unpaired t test.

(E) Western blots with indicated antibodies of CAL1 IPs from chromatin extracts digested with either DNase or MNase. IN, input; M, mock (IP with beads only).

transcript levels displayed a decrease at 8 hr post-induction that was also observed in an independent time course experiment (Figure S1A). This transient dip likely reflects the kinetics of induction of the MT promoter (Bunch et al., 1988) driving CAL1-GFP-LacI. Detection of nascent lacO^b transcripts showed they are produced continuously, reaching a peak from 24–30 hr after induction (Figures S1B and S1C), a time during which it is expected that most lacO cells have acquired CENP-A at the lacO site (Figure 1C). Thus, we reveal a striking correlation between transcription and CENP-A incorporation at the lacO site.

To ensure that transcription of lacO^b is not due to the addition of $CuSO_4$ or is not somehow linked to the binding of the GFP-LacI fusion protein to the lacO array, we carried out qRT-PCR comparisons in the presence or absence of $CuSO_4$ between the following cell lines: CAL1-GFP-LacI cells, GFP-LacI cells, and cells completely lacking any *LacI* transgene, yet still harboring the integrated lacO plasmid (lacO). These experiments showed that transcription from lacO^b was only observed in induced CAL1-GFP-LacI cells (Figure 1E). No lacO^b transcription was detected in induced cells containing CAL1-GFP-LacI or GFP-LacI without lacO (data not shown).

The expression of a control gene, *actin*, which is transcribed by RNAPII, was unaffected, suggesting that addition of $CuSO_4$ does not cause non-specific transcriptional upregulation (Figure S1D). An increase in transcription from lacO^b was also observed when the lacO plasmid was introduced episomally, along with the CAL1-GFP-LacI plasmid, via transient transfection in S2 cells (Figure 1F). These transient transfections displayed low efficiency (~12%, as estimated by IF with anti-GFP antibodies, data not shown), resulting in fewer transcripts being detected by qRT-PCR compared to stable cells. Nonetheless, they demonstrate that transcription of lacO^b occurs independently of its chromosomal insertion.

Transcription of lacO^b Correlates with CENP-A and RNAPII Distribution

To gain more insight into the relationship between transcription and CENP-A occupancy across the lacO locus, we performed paired-end RNA sequencing (RNA-seq) and chromatin immunoprecipitation sequencing (ChIP-seq) experiments. RNA-seq of induced CAL1-GFP-LacI cells revealed that 28.5 fragments per million (fpm) mapped to lacO^b, whereas only 0.45 fpm mapped to the lacO array itself, where CAL1 is tethered. This could be due to blockage of RNAP passage by LacI bound to lacO repeats (Jacob and Monod, 1961). Thus, upon CAL1-GFP-LacI induction, most of the transcription originates from lacO^b sequences. Consistent with our qRT-PCR results (Figures 1D–1F), induced GFP-LacI cells displayed fewer reads mapping to lacO^b (12.8 fpm; $p < 0.05$; Figure 2A).

CENP-A ChIP-seq of induced CAL1-GFP-LacI cells revealed a preferential association of CENP-A with the lacO^b versus the lacO array (4,751.6 versus 2,462.5 fpm; Figures 2B and 2C). Since GFP ChIP-qPCR showed that CAL1-GFP-LacI is also enriched at lacO^b (Figure 2D), we concluded that CENP-A and CAL1-GFP-LacI spread to lacO^b from the lacO array, where CAL1-GFP-LacI is initially tethered.

Active RNAPII localizes to the centromeres of metaphase chromosomes in *Drosophila* (Rošić et al., 2014), raising the possibility that RNAPII may mediate transcription of lacO^b upon CAL1-GFP-LacI tethering. ChIP-seq with antibodies specific for the elongating form of RNAPII (RNAPIIS2p) showed a marked increase in RNAPIIS2p occupancy at the lacO^b after CAL1-GFP-LacI induction (178.3 fpm versus 75.5 fpm), suggesting that RNAPII mediates lacO^b transcription. Furthermore, the distribution of RNAPIIS2p closely resembled that of CENP-A in induced cells, with low occupancy on the lacO array and higher occupancy on the lacO^b array (32.3 versus 178.3 fpm; Figures 2B–2C), consistent with a

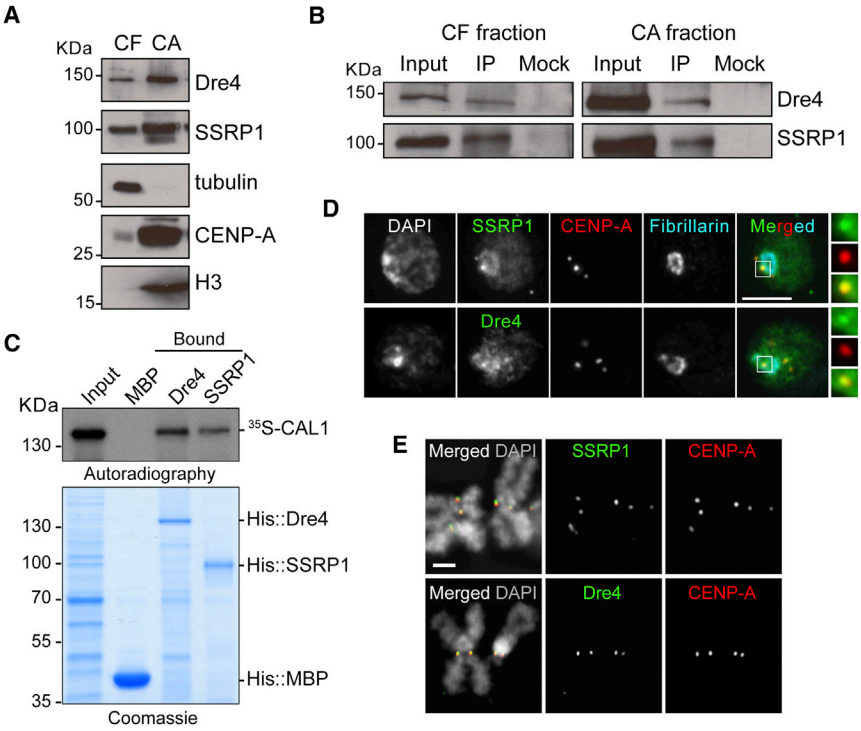

Figure 3. FACT Interacts with CAL1 and Localizes to the Centromere in S2 Cells

(A) Western blots of chromatin-free (CF) and chromatin-associated (CA) extracts from S2 cells with indicated antibodies. Tubulin and histone H3 antibodies are positive controls for their respective fractions.

(B) Western blots of IPs with anti-CAL1 antibodies from CF and CA extracts. Mock are IPs with rabbit immunoglobulin G (IgG).

(C) Direct interaction between in-vitro-translated ^{35}S-methionine-labeled CAL1 with recombinant His::Dre4 or His::SSRP1 bound to Ni-NTA beads. His::MBP, negative control.

(D) IF with anti-SSRP1 or anti-Dre4 (green), anti-CENP-A (red), and anti-fibrillarin (blue) antibodies. DAPI shown in gray. Insets show 3× magnifications of boxed centromere. Scale bar, 5 μm.

(E) IF on metaphase chromosomes with anti-SSRP1 or anti-Dre4 (green) and anti-CENP-A (red) antibodies. DAPI shown in gray. Scale bar, 1 μm.

See also Figure S2 and Table S1.

functional interplay between CENP-A assembly and transcriptional activity.

Low levels of CENP-A and RNAPIIS2p were observed in uninduced CAL1-GFP-LacI cells (Figure 2B), possibly due to leaky expression of CAL1-GFP-LacI, but these were found to be significantly lower than in induced samples ($p < 0.001$ and $q < 0.001$ for both CENP-A and RNAPIIS2p ChIPs; see the Supplemental Experimental Procedures; ChIP-seq and RNA-seq mapping).

Interestingly, immunoprecipitation (IP) of chromatin-associated CAL1 revealed a physical association between CAL1 and RNAPIIS2p (Figure 2E). This interaction and our ChIP-seq results indicate that CAL1 recruits RNAPIIS2p onto chromatin, in turn stimulating transcription. Why only a subset of the RNAPIIS2p-associated sequences produced transcripts by RNA-seq remains unclear. It is possible that some of these transcripts are unstable and cannot be detected by this type of assay.

Isolation of FACT, a CAL1 Interactor

Having shown that targeting of CAL1 to lacO triggers accumulation of RNAPIIS2p and transcription, we sought to identify the key components of this process by isolating CAL1-interacting factors. We performed IPs of FLAG-tagged CAL1 (Chen et al., 2012) from chromatin-free (CF) and chromatin-associated (CA) cell extracts with anti-FLAG- M_2 agarose beads, using *Drosophila* S2 cells (no FLAG tag) as a negative control. Mass spectrometric analysis (see Table S1; data not shown) identified among the highest scoring unique hits Spt16 (called Dre4 in *Drosophila*) and SSRP1, the two subunits of the heterodimeric FACT complex (Orphanides et al., 1999). FACT allows the progression of the transcriptional machinery through chromatinized templates (Belotserkovskaya et al., 2003; Orphanides et al., 1999), by a mechanism involving nucleosome destabilization (Hondele and Ladurner, 2013; Hondele et al., 2013), and was found to be associated with human CENP-A (Foltz et al., 2006), and to be important for CENP-A localization in chickens (Okada et al., 2009). Thus, FACT is a strong candidate for mediating CENP-A deposition-coupled transcription.

In order to confirm the association between CAL1 and the FACT complex, CF and CA fractions were prepared from S2 cells, and CAL1 IPs were performed using anti-CAL1 antibodies. Dre4 and SSRP1 were present in both fractions (Figure 3A) and associated with CAL1 in both cases (Figure 3B), confirming our proteomic results. Reciprocal IPs were performed using anti-FLAG antibodies to precipitate FLAG-Dre4 or FLAG-SSRP1; however, CAL1 was not detected (Figure S2A), suggesting that only a small fraction of FACT interacts with CAL1.

Next, we sought to determine if the association between CAL1, Dre4, and SSRP1 is direct by analyzing protein-protein interactions between recombinant His-Dre4 or His-SSPR1 and in-vitro-translated ^{35}S-methionine-labeled CAL1. The His-Dre4 and His-SSRP1 proteins heterodimerized in vitro (Figure S2B), suggesting that they are properly folded, and both pulled down CAL1 (Figure 3C), demonstrating direct interaction.

FACT is involved in RNAPII (Belotserkovskaya et al., 2003; Krogan et al., 2002; LeRoy et al., 1998; Orphanides et al., 1998), RNAPI, and RNAPIII transcription (Birch et al., 2009); therefore, it is expected to be broadly distributed throughout chromatin. To determine if FACT displays any centromeric enrichment, we used IF with anti-Dre4 and anti-SSRP1 antibodies. After extraction with detergent pre-fixation, a treatment expected to remove loosely chromatin-bound proteins, FACT was enriched at interphase centromeres (identified by CENP-A staining) and at the nucleolus (identified by Fibrillarin staining; Figure 3D). Examination of FACT localization on metaphase chromosome spreads revealed an even more striking centromeric accumulation of Dre4 and SSRP1, demonstrating that during mitosis, when active deposition of newly synthesized

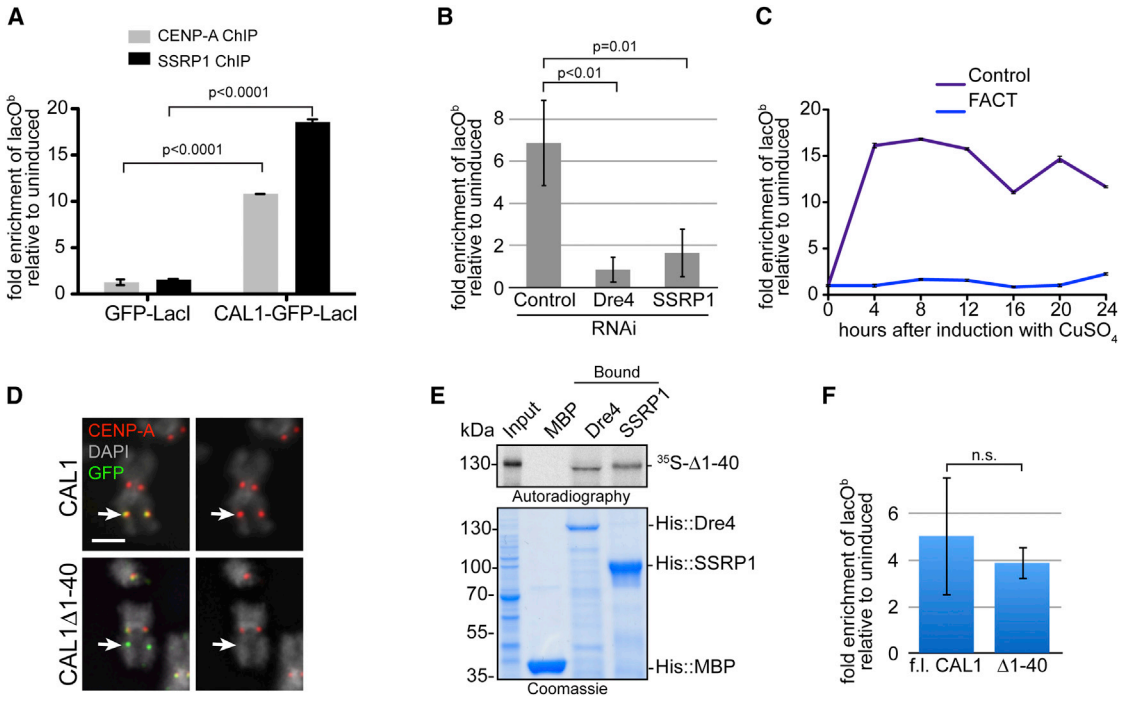

Figure 4. FACT Is Required for CENP-A Deposition-Coupled Transcription

(A) CENP-A and SSRP1 ChIP-qPCR in CAL1-GFP-LacI and GFP-LacI lacO cells. The graph shows the enrichment of induced cells (24 hr) relative to uninduced cells. Error bars, 95% CI of three technical replicates. Significant p values (unpaired t test) are shown.

(B) qRT-PCR of lacO^b transcripts in CAL1-GFP-LacI cells induced (24 hr) 6 days after the indicated RNAi treatments. p values (unpaired t test) are shown. The means ± SD of three experiments are shown.

(C) qRT-PCR of lacO^b transcripts in control (purple) and SSRP1/Dre4 RNAi (blue) cells at the indicated times. Error bars, SD of three technical replicates.

(D) IF with anti-CENP-A (red) and anti-GFP (green) antibodies in lacO cells expressing full-length CAL1-GFP-LacI (top) or CAL1Δ1-40-GFP-LacI (bottom). DAPI is shown in gray. Arrow points to the lacO site. Scale bar, 1 μm.

(E) Direct interaction between in-vitro-translated ^{35}S-methionine-labeled CAL1Δ1-40 (^{35}S-Δ1-40) with recombinant His::Dre4 (Dre4) or His::SSRP1 (SSRP1) bound to Ni-NTA beads. His::MBP (MBP) is a negative control.

(F) qRT-PCR of lacO^b transcripts in induced cells (24 hr) transiently expressing full-length (fl) CAL1-GFP-LacI or CAL1Δ1-40-GFP-LacI. Means ± SEM of three experiments are shown. p = 0.68 (not significant; unpaired t test).

CENP-A takes place (Mellone et al., 2011), FACT is more strongly associated with the centromere than with other regions of the genome (Figure 3E). These results were confirmed with epitope tagged SSRP1 and Dre4 (data not shown) and are consistent with a previous study in chicken DT-40 cells (Okada et al., 2009).

The Transcription Associated with CENP-A Deposition Requires FACT

Given that FACT enables RNAP progression, we next investigated whether FACT is required for the transcription we observed during CAL1-mediated CENP-A assembly at the lacO site. First, we investigated if CAL1-GFP-LacI recruits FACT to lacO^b using ChIP-qPCR with anti-SSRP1 antibodies (Nakayama et al., 2007). CENP-A ChIPs were performed in parallel. CAL1-GFP-LacI or GFP-LacI (negative control) cells were induced for 24 hr. CENP-A and SSRP1 were both found to be enriched in induced CAL1-GFP-LacI cells (Figure 4A). We concluded that FACT is recruited by CAL1-GFP-LacI to lacO^b.

Next, we measured lacO^b transcription by qRT-PCR after induction of CAL1-GFP-LacI cells, in which Dre4 and SSRP1 had been knocked down by RNAi for 6 days. Control cells displayed, on average, a 6.8-fold increase in lacO^b transcript levels 24 hr after induction with $CuSO_4$. In contrast, cells lacking FACT showed virtually no increase (Figure 4B). This result was also confirmed in a time course experiment, in which, after 6 days of FACT RNAi, CAL1-GFP-LacI was induced and qRT-PCR was performed on RNA extracted every 4 hr for 24 hr (Figure 4C). Together, these data demonstrate that FACT is required for the transcription observed upon CAL1 targeting.

CAL1-directed transcription could be a by-product of CENP-A incorporation, or it could occur independently of CENP-A deposition through the recruitment of RNAPII and FACT onto chromatin. To distinguish between these two possibilities, we used a CAL1 mutation lacking a short Scm3-like domain (Phansalkar et al., 2012; CAL1Δ1-40), which is defective in recruiting CENP-A to the lacO (Figure 4D; Chen et al., 2014). Importantly, CAL1Δ1-40 can interact directly with Dre4 and SSRP1 (Figure 4E). When we tethered CAL1Δ1-40-GFP-LacI to the lacO, we observed levels of lacO^b transcription indistinguishable from those initiated by CAL1-GFP-LacI (Figure 4F). We concluded that lacO^b transcription depends on CAL1 and FACT, but it does not require CENP-A incorporation.

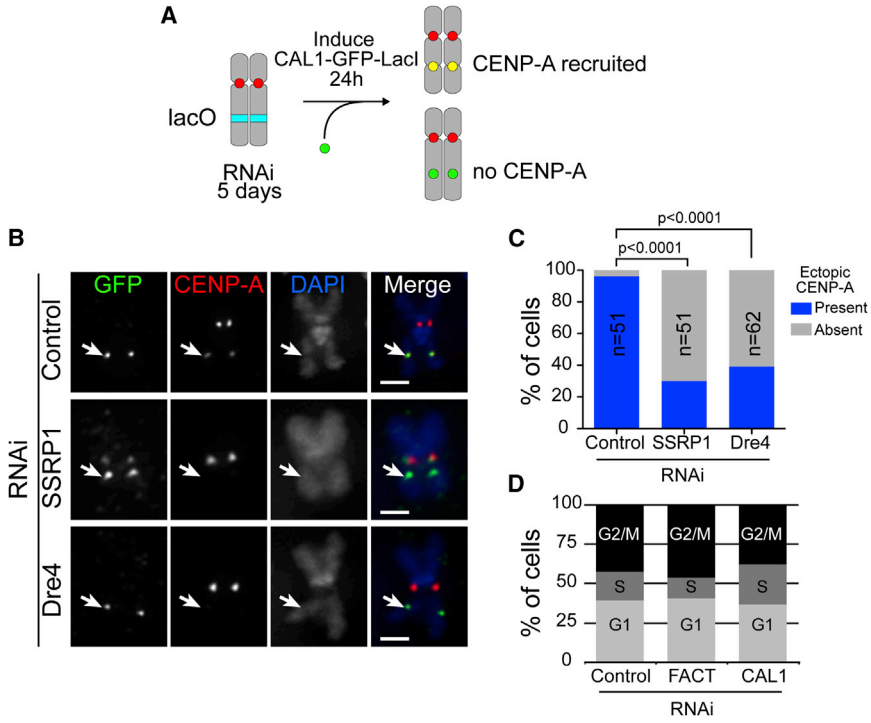

Figure 5. FACT Is Required for the De Novo Incorporation of CENP-A at an Ectopic Locus

(A) Cartoon depicting the experimental strategy to assess de novo CENP-A recruitment in the absence of FACT.

(B) lacO CAL1-GFP-LacI cells were subjected to RNAi to deplete Dre4, SSRP1, or a control for 5 days, followed by induction with $CuSO_4$ for 24 hr. Metaphase chromosome spreads were stained with anti-GFP (green) and anti-CENP-A antibodies (red). DNA was stained with DAPI (blue).

(C) Graph showing the percentage of CAL1-GFP-LacI-positive cells in which ectopic CENP-A signal was present or absent. Bars, 1 μm. $p < 0.0001$ (chi-square test).

(D) FACS profile of control, CAL1, and SSRP1/Dre4 (FACT) RNAi cells.

See also Figure S3 and Table S2.

FACT-Mediated Transcription Is Required for De Novo CENP-A Incorporation

CAL1 binds directly to FACT and recruits FACT and RNAPII to sites of CENP-A assembly. To determine if the absence of lacO[b] transcription caused by knockdown of FACT affects deposition of CENP-A at the lacO site, we depleted Dre4 or SSRP1 by RNAi for 5 days, induced CAL1-GFP-LacI for 24 hr, and performed IF with anti-CENP-A and anti-GFP antibodies on metaphase spreads (Figure 5A). Ectopic targeting of CAL1 via LacI/lacO leads to efficient de novo incorporation of CENP-A (Chen et al., 2014). In contrast, depletion of either SSRP1 or Dre4 resulted in a significant reduction in the percentage of CENP-A-positive lacO sites (Figures 5B and 5C). Since FACT depletion did not affect the formation of the CENP-A/CENP-C/CAL1 complex (Erhardt et al., 2008; Figure S3A), a defect in CENP-A incorporation is the most likely explanation for this reduction in ectopic CENP-A. Thus, these experiments demonstrate that efficient recruitment of CENP-A by CAL1 requires FACT and imply that CAL1 is not sufficient to assemble CENP-A into nucleosomes when chromatin is the substrate, as opposed to when naked DNA is the substrate (Chen et al., 2014).

Given the ubiquitous role of FACT in DNA metabolism, we investigated possible pleiotropic effects that could account for the CENP-A incorporation defect seen after FACT RNAi. Fluorescence-activated cell sorting (FACS) analysis showed no change in the distribution of cells in G1, S, or G2-M upon FACT RNAi (Figure 5D), suggesting that the CENP-A incorporation defect is not due to a cell-cycle defect. Additionally, qRT-PCR analyses of *cenp-a*, *cal1*, or *cenp-c* transcripts (Figures S3B and S3C) and western blot analyses from total protein extracts (Figure S3D) demonstrated that FACT depletion did not decrease the expression of these essential centromere genes. Similarly, expression of eight handpicked genes that are bound to Dre4 based on ChIP-chip data (Kharchenko et al., 2011; Table S2), as well as that of the FACT-associated gene Hsp70 (Saunders et al., 2003), did not decrease upon FACT RNAi. This suggests that general transcription involves redundant chromatin remodeling activities, at least in *Drosophila*-cultured cells. Altogether, these results demonstrate that FACT plays a specific function in CENP-A deposition.

Depletion of FACT Causes Defective CENP-A Recruitment at Endogenous Centromeres

To determine if FACT is required for the recruitment of newly synthesized CENP-A at endogenous centromeres, we performed quench-chase-pulse experiments in cells stably expressing SNAP-tagged CENP-A (Jansen et al., 2007; Mellone et al., 2011). FACT was knocked down by simultaneous RNAi of Dre4 and SSRP1 for 6 days, after which time pre-existing SNAP-tagged CENP-A was irreversibly quenched using the BG-blocking agent (T_0; quench). RNAi of CAL1 was used as a positive control. After a chase that lasted until cells had divided once, newly synthesized SNAP-tagged CENP-A was labeled using TMR* (T_1; pulse) and cells were fixed and processed for IF (Figure 6A). Immediately after quenching SNAP-CENP-A, no TMR*-labeled CENP-A signal was observed, as expected, while labeling with an anti-CENP-A antibody showed that low levels of CENP-A were still present in both FACT and CAL1 RNAi (Figure 6B, T_0). After one cell division, cells were incubated with TMR* to label newly synthesized SNAP-CENP-A. Newly synthesized SNAP-CENP-A was clearly visible at the centromeres of control cells (Figure 6B, T_1, top). In contrast, there was a significant drop in the TMR*-CENP-A intensity levels of FACT RNAi cells, consistent with defective CENP-A recruitment (Figures 6B, T_1, and 6C).

To determine if FACT is also required to retain pre-existing centromeric CENP-A through one cell division, we quantified the total centromeric CENP-A IF signal at T_0 and T_1. In control cells, retention and recruitment of CENP-A are intact; therefore, no change in total CENP-A intensity occurs over one cell

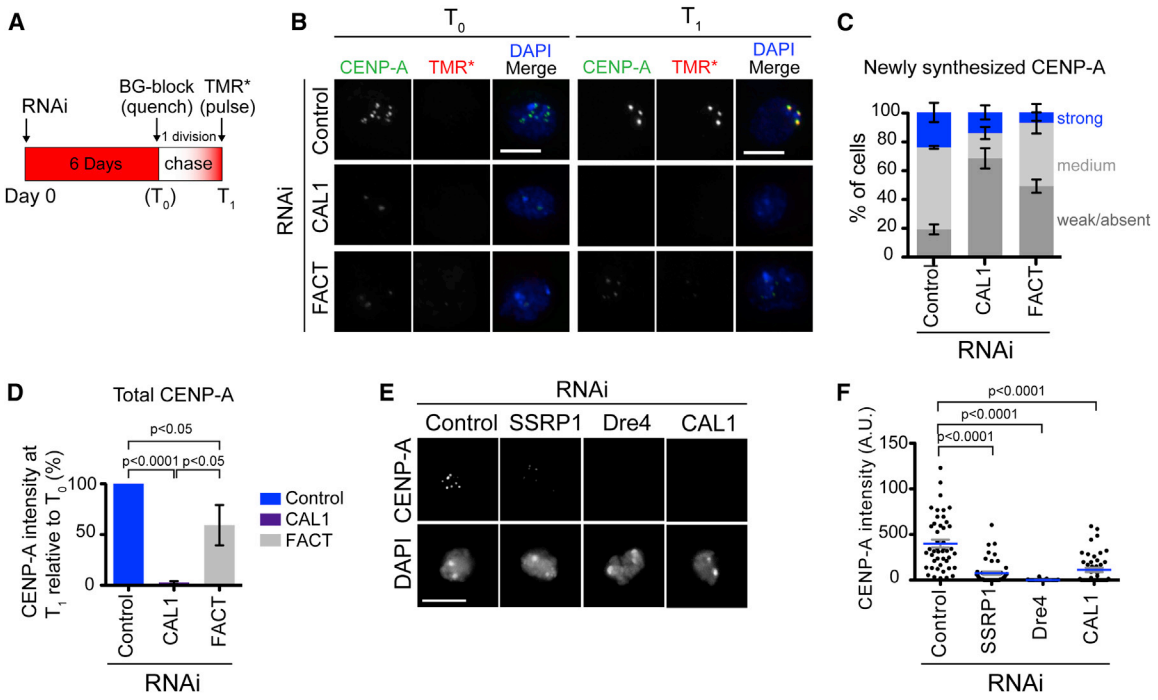

Figure 6. FACT Is Required for CENP-A Recruitment at Endogenous Centromeres

(A) Diagram of the quench-chase-pulse experiment.

(B) IF with anti-CENP-A antibodies (green) in control and Dre4/SSRP1 RNAi SNAP-CENP-A cells pulsed with TMR* (red) immediately after BG-block (T_0, left) or after having completed one cell division (T_1, right). DAPI is shown in blue. Scale bars, 5 μm.

(C) Quantification of the signal intensity of TMR*-labeled CENP-A foci. The means ± SEM of three experiments (100 cells quantified per RNAi treatment) are shown. $p < 0.0001$ for control versus SSRP1/Dre4 RNAi (unpaired t test).

(D) The total CENP-A centromeric intensity for control cells, CAL1 RNAi cells, and SSRP1/Dre4 RNAi (FACT) was quantified at T_0 and T_1. The mean change in CENP-A intensity at T_1 relative to T_0 ± SEM is shown. n = 3 experiments (150 cells each RNAi treatment). p values from an unpaired t test are shown.

(E) IF with anti-CENP-A antibodies of S2 cells subjected to the indicated RNAi treatments. DNA is stained with DAPI. Scale bar, 5 μm.

(F) Scatter plot showing total centromeric CENP-A signal intensity per cell from the experiment in (E). n = 50 cells per condition. p values from an unpaired t test are shown.

See also Figure S4.

division (T_1/T_0 = 100%). In contrast, in cells lacking FACT, centromeric CENP-A signal displayed a decrease in intensity consistent with a loading defect (T_1/T_0 = ~59%; Figure 6D; a ratio lower that 50% would be expected if the retention of pre-existing CENP-A were also affected). These results also explain why CENP-A is lost at a relatively slower rate in the absence of FACT (6 days): its loading is compromised but its retention is not. In contrast, loss of CENP-A from the centromere in the absence of CAL1 is much more rapid (Figure 6D), consistent with the dual role of CAL1 in CENP-A loading and stabilization from degradation (Chen et al., 2014). Collectively, our data demonstrate that FACT is required for the centromeric recruitment of newly synthesized CENP-A at the centromere.

To examine if FACT depletion can lead to complete loss of CENP-A from centromeres, we knocked down Dre4 or SSRP1, transfecting S2 cells twice with double-stranded RNA (dsRNA) over 6 days and examined the intensity of centromeric CENP-A by IF. We observed a dramatic decrease in the intensity of CENP-A foci upon Dre4 or SSRP1 RNAi compared to control cells (Figures 6E and 6F), demonstrating that two consecutive RNAi lead to a nearly complete loss of CENP-A from centromeres. Consistent with defective CENP-A recruitment, we observed a significant increase in chromosome missegregation in mitosis in cells lacking FACT (Figure S4).

H3.1 and H3.3 Accumulate within Centromeric Chromatin upon FACT RNAi

In human cells, histone H3 nucleosomes are deposited in S phase as temporary placeholders that need to be replaced by CENP-A in order to maintain centromere identity (Dunleavy et al., 2011). Whether CENP-A chaperones or other factors perform this exchange is unknown. Transcription at the centromere could mediate the eviction of the placeholder H3 during CAL1-mediated CENP-A deposition, analogously to H3.3 deposition at active genes (Schwartz and Ahmad, 2005). To determine if, in the absence of FACT and transcription, histone H3.1 or H3.3 accumulate at centromeres, we depleted Dre4 (which causes loss of SSRP1 as well; Figure S5) in S2 cells transiently transfected with plasmids expressing V5-tagged H3.1 and H3.3 and inspected centromeric chromatin by IF on stretched chromatin fibers. In Dre4-depleted cells, the average length of continuous CENP-A fibers was about one-half that of control cells (Figure 7A) and the CENP-A signal became less contiguous, suggesting that

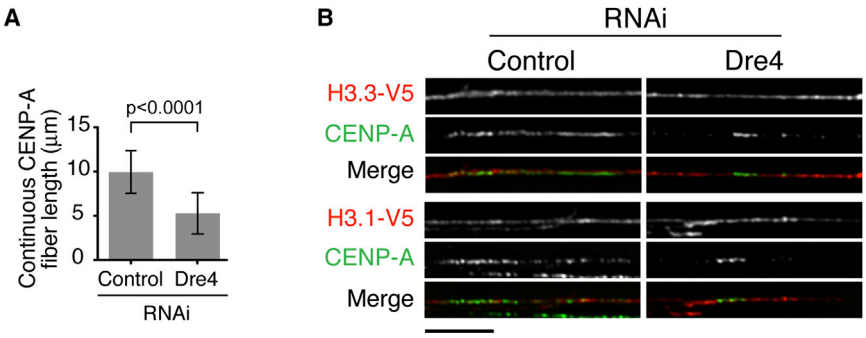

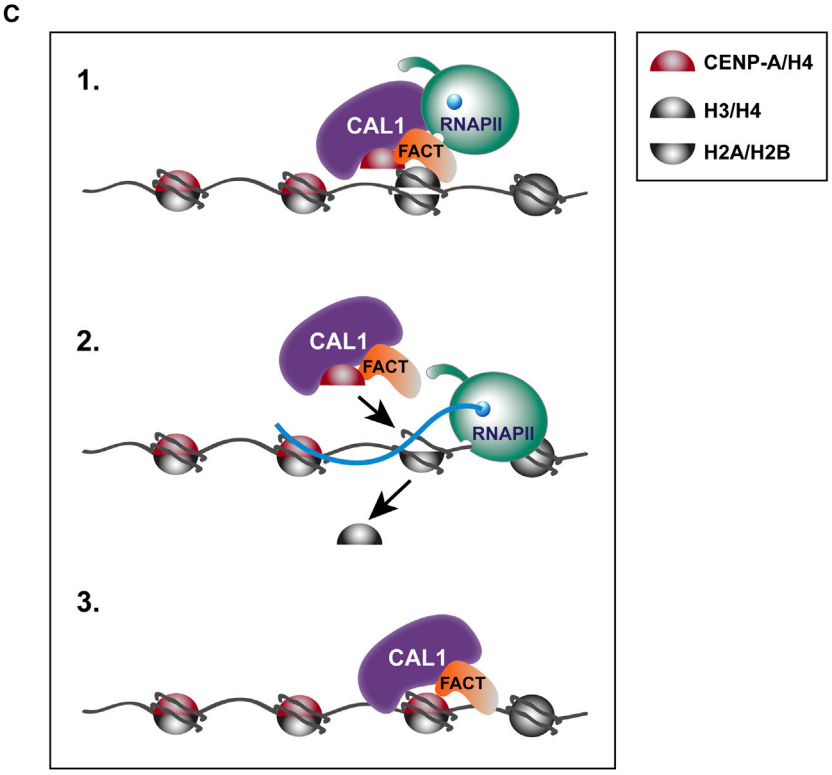

Figure 7. FACT Depletion Results in Accumulation of Histone H3-Containing Nucleosomes within Centromeric Chromatin

(A) Quantification of CENP-A fiber length from three experiments (n = 74 total fibers per condition). The means ± SD are shown. $p < 0.0001$ for control versus each RNAi (unpaired t test).

(B) IF on stretched chromatin fibers from control and Dre4 RNAi S2 cells expressing H3.1-V5 or H3.3-V5. V5 shown in red and CENP-A in green (n = 10–17 fibers per condition). Scale bar, 5 μm.

(C) Model for the role of RNAPII transcription in centromere propagation. FACT is recruited to the centromere along with CAL1 and CENP-A/H4; here, it destabilizes H3-containing nucleosomes, allowing the passage of RNAPII through chromatin (1). RNAPII transcribes through the region causing the eviction of H3/H4 tetramers (2), thereby allowing deposition of new CENP-A/H4 tetramers (3).

CENP-A is lost throughout CENP-A centromeric chromatin stretches, as well as from their edges. IF with anti-CENP-A and anti-V5 antibodies showed that H3.1 and H3.3 were continuously present across CENP-A fibers in control and RNAi cells, indicating that upon loss of CENP-A, no "gaps" were left at the centromere (Figure 7B). These results, which are consistent with a previous study that looked at centromeric fibers upon CENP-A depletion (Blower et al., 2002), suggest defective exchange between the placeholders H3.1/H3.3 and CENP-A in the absence of FACT and transcription.

Collectively, our data suggest a model in which FACT is recruited to the centromere by interacting directly with CAL1 in a pre-nucleosomal complex. Once at the centromere, FACT destabilizes nucleosomes (Hondele and Ladurner, 2013; Hondele et al., 2013), allowing transcription through the region via RNAPII. Finally, transcription by RNAPII causes the eviction of the placeholders H3.1 and H3.3, allowing the deposition of CENP-A by CAL1 (Figure 7C).

DISCUSSION

The epigenetic maintenance of centromeres through faithful CENP-A deposition is a process crucial for genome stability. Much of the recent advances in understanding this process in metazoans have focused on the dissection of the specific proteins involved in CENP-A recruitment. In contrast, the roles of DNA and chromatin in CENP-A deposition have remained largely elusive. In this study, we have uncovered a key role for transcription in *Drosophila* CENP-A deposition and have identified FACT as a central player in this process. This mechanism of nucleosome reorganization—combining RNAPII passage with CENP-A/H3 exchange—is analogous to other paradigms seen during transcription and development. For example, FACT is recruited to specific genomic loci by the GAGA factor, where it destabilizes nucleosomes, allowing replacement of histone H3.1 with H3.3 by the chaperone HIRA and thereby modulating the expression of *Hox* genes (Nakayama et al., 2007; Shimojima et al., 2003).

To ensure the fidelity of centromere propagation, CENP-A chromatin must be replenished after each round of DNA replication. In human cells, newly synthesized CENP-A is recruited to centromeric chromatin along with newly synthesized histone H4, indicating that CENP-A and H4 form a sub-nucleosomal core, which is assembled simultaneously (Bodor et al., 2013). As such, it is conceivable that CENP-A/H4 deposition involves the eviction of pre-existing H3/H4 tetramers.

To determine if CENP-A assembly is coupled to transcription, we used an inducible ectopic centromere system in *Drosophila* S2 cells. We discovered that a remarkable change in transcription occurs rapidly upon CAL1-GFP-LacI targeting at the lacO site. The same DNA that is transcribed is enriched in RNAPII,

suggesting that this polymerase is the one mediating this transcription. The interaction between CAL1 and RNAPII supports this idea, although the involvement of additional RNAPs cannot be ruled out.

In order to characterize this phenomenon mechanistically, we biochemically isolated the CAL1 partner FACT and demonstrated that it is necessary for the transcription of the lacO site. Despite its function in global RNAP elongation, the depletion of FACT did not cause a decrease in expression of FACT-associated genes, suggesting a redundancy of mechanisms directing general transcription in *Drosophila* cells. In contrast, upon FACT RNAi, transcription at the lacO site was impaired, resulting in defective de novo CENP-A deposition, demonstrating a specific disruption of centromere chromatin assembly.

Surprisingly, we found that transcription at the lacO site is independent of CENP-A assembly, revealing that CENP-A chaperones can initiate local chromatin reorganization through the recruitment of FACT and RNAPII.

The discovery that chromatin poses a barrier to CENP-A deposition by its chaperone and the involvement of FACT-mediated transcription in overcoming this barrier is likely to be relevant to other complex eukaryotes. In budding yeast, FACT allows Phs1 to access misincorporated CENP-A/Cse4 nucleosomes, allowing the ubiquitylation and subsequent degradation of CENP-A/Cse4 (Deyter and Biggins, 2014). However, our studies in *Drosophila* demonstrate that FACT is directly implicated in CENP-A deposition. The finding that FACT is required for CENP-A localization in chicken (Okada et al., 2009) and interacts with human CENP-A (Foltz et al., 2006) raises the possibility that the mechanism by which FACT promotes chromatin reorganization during CENP-A deposition by its chaperone may be conserved from flies to vertebrates.

In budding yeast, FACT increases nucleosome accessibility to nucleases in the absence of H2A-H2B dimer displacement, suggesting that it can reorganize nucleosomes in a more open configuration, while maintaining their original composition (Xin et al., 2009). Consistent with this, the crystal structure and mutational analyses of Spt16/Dre4 showed that FACT allows a gradual invasion of the nucleosome, breaking strong octamer-DNA contacts and allowing the passage of polymerases (Hondele et al., 2013). Thus, FACT is likely to function as a nucleosome destabilizer (Hondele and Ladurner, 2013), allowing the passage of RNAPII, which in turn interacts with CAL1 (Figure 7C).

A question that remains unanswered is whether the transcripts produced during CENP-A deposition are simply a by-product of the ongoing chromatin reorganization or if they are necessary components of centromere structure and identity. Specific RNAs emanating from centromeres do appear to play a role in centromere/kinetochore integrity (Carone et al., 2013; Quénet and Dalal, 2014; Rošić et al., 2014; Topp et al., 2004). However, the sequence requirements of these RNAs remain poorly defined. Our work demonstrates a requirement for transcription in CENP-A deposition as a means to reorganize nucleosomes and suggests the dispensability of specific centromeric RNA sequences in this process. Either there is a generic, non-sequence specific role for RNA at the centromere or specific sequences emanating from the centromere possess additional structural properties. Further work is needed to elucidate the functional relationship between CENP-A deposition-coupled transcription and structural centromeric RNAs.

EXPERIMENTAL PROCEDURES

Large-Scale Immunoprecipitation and Mass Spectrometry

FLAG-CAL1 complexes were purified from chromatin-free extracts generated from 2×10^9 S2 cells, as described previously (Chen et al., 2012; Mellone et al., 2011). FLAG-CAL1 complexes from chromatin-associated complexes were generated by homogenization, nuclear extraction, and digestion with benzonase. Extracts were added to anti-FLAG M2 beads (Sigma-Aldrich). After washing, complexes were eluted with FLAG peptide (Sigma-Aldrich) and sent for mass spectrometric analysis (see the Supplemental Experimental Procedures for details).

Small-Scale Immunoprecipitations

Extracts from chromatin-free and chromatin-associated fractions were prepared from 10^8 cells, as described before (Mellone et al., 2011). Extracts were added to Dynabeads-protein A beads (Life Technologies) coupled with anti-CAL1 or anti-FLAG antibodies (Sigma-Aldrich) and incubated for 10 min at room temperature, followed by a 30 min incubation at 4°C with rotation. Beads were washed three times with PBS-T (PBS; 0.1% Triton). 6% of the input and 50% of the IP was analyzed by 10% SDS-PAGE, followed by western blot. See the Supplemental Experimental Procedures for CAL1/RNAPII IPs.

In Vitro Protein Binding Assay

All steps were performed at room temperature. ~5 μg of purified His::MBP (negative control) and His::Dre4 or His::SSRP1 immobilized on Ni-NTA agarose (QIAGEN) were equilibrated in binding buffer containing 50 mM HEPES (pH 7.4), 150 mM NaCl, 1 mM $MgCl_2$, 1 mM EGTA, 0.1% Triton X-100, 1× EDTA-free protease inhibitor cocktail (Roche), 20 mM imidazole, and 0.5 mg/ml BSA, mixed with ^{35}S-methionine-labeled proteins expressed by a coupled in vitro transcription translation system (IVTT), and incubated for 1 hr. Beads were then washed in binding buffer (without BSA); proteins were eluted by boiling in Laemmli sample buffer and subjected to SDS-PAGE, followed by autoradiography. See also the Supplemental Experimental Procedures.

Cell Culture and RNAi

Stable S2 cells containing an integrated lacO plasmid (pAFS52; Straight et al., 1996) were described before (Chen et al., 2014; Mendiburo et al., 2011). Additional stable S2 cells were generated by transfection with Cellfectin reagent (Life Technologies) and selection with 450 μg/ml hygromycin. Stable lacO S2 cells were re-thawed after 1 month in culture due to loss of the lacO array over time. Transient transfections were performed by treating cells with FuGENE HD (Promega) for 2 days. Cells were induced with 0.5 mM $CuSO_4$ for 24 hr.

Stable CAL1-GFP-LacI or GFP-LacI cells were induced with 0.5 mM $CuSO_4$ at 25°C for 1–48 hr or left uninduced. RNAi was performed using DOTAP and 10 μg of dsRNA (see the Supplemental Experimental Procedures).

Total RNA Extraction and qRT-PCR

Total RNA was isolated from 1×10^7 cells using TRI-reagent (Sigma-Aldrich). 10 μg of RNA was treated with 1 μl of Turbo DNase (Life Technologies) for 30 min at 37°C. RNA was reverse transcribed using the iScript cDNA Synthesis Kit (Bio-Rad), and 2 μl were used in qPCR using SYBR-green (Bio-Rad) on a CFX96 Real-Time System (Bio-Rad). Transcription from the $lacO^b$ (using primer pairs 1.6 or 3; Mendiburo et al., 2011) was normalized to uninduced samples. Values were calculated using the Pfaffl method (Pfaffl, 2001), with Rp49 (unaffected by FACT; Nakayama et al., 2007) as a reference gene. Some variability in the fold increase in $lacO^b$ transcription between experiments was observed due to instability of the lacO array during cell culture over time. See the Supplemental Experimental Procedures for primer sequences.

For RNA-seq, libraries were generated using the Tru-Seq kit (Illumina) and ran on a HiSeq. See the Supplemental Experimental Procedures for mapping information.

Total Protein Extraction and Western Blotting

Total cell extracts were obtained from 1 × 10^6 cells resuspended in 15 μl of RIPA buffer (150 mM NaCl, 50 mM Tris [pH 8], 1% NP40, and 0.1% SDS), incubated on ice for 10 min, and digested with 1 μl of benzonase (Novagen) for 20 min at 37°C. Extracts were separated by 10% SDS-PAGE and transferred to nitrocellulose membranes. After 30 min incubation in blocking buffer (TBS, 0.1% Tween 20, 5% powder non-fat milk), membranes were incubated overnight at 4°C with anti-CAL1 (rabbit, 1:1,000; from A. Straight), anti-CENP-A (rabbit, 1:1,000; Active Motif), anti-FLAG (mouse, 1:1,000; Sigma-Aldrich), anti-Dre4 and anti-SSRP1 (rabbit, 1:1,000; from S. Hirose), and anti-RNAPIIS2p (mouse, 1:1,000; Abcam); anti-CENP-C (guinea pig, 1:3,000; Mellone et al., 2011), anti-tubulin (mouse, 1:1,000; Sigma-Aldrich), or anti-histone H3 (rabbit, 1:5,000; Abcam) antibodies were used as a loading control.

Immunofluorescence

IF on settled cells and metaphase spreads was performed as described (Chen et al., 2014). For pre-extraction with detergent, settled cells were immersed in 100 μl of PBS-T for 5 min, followed by the addition of 11 μl of 37% formaldehyde for 10 min. Stretched chromatin fibers were performed essentially as described (Sullivan, 2010), using twice the amount of primary antibodies than conventional IF. Only extensively stretched fibers (DAPI nearly undetectable) were used for our analyses. The antibodies used were anti-CENP-A (chicken, 1:1,000; Blower and Karpen, 2001), anti-GFP (rabbit-488 conjugated, 1:100; Life Technologies), anti-CENP-C (guinea pig, 1:1,000; Mellone et al., 2011), anti-fibrillarin (mouse, 1:500; Cytoskeleton), and anti-V5 (mouse, 1:50; Life Technologies). Secondary antibodies (Life Technologies Alexa-Fluor 488 or 546 conjugated; Santa Cruz biotechnology CY5 conjugated; 1:500) were used as appropriate. Slides were mounted in Slowfade (Life Technologies) containing DAPI.

Quench-Pulse-Chase Assay

RNAi of both Dre4 and SSRP1 was simultaneously performed for 6 days in a 12-well plate. Quench-chase-pulse, followed by IF, was performed as described (Mellone et al., 2011), making sure the cells had divided once (~24 hr for control and 24–48 hr for FACT RNAi) between BG-block (quench) and TMR* labeling (chase).

Fluorescence-Activated Cell Sorting

After 6 days of RNAi (Bw for control and SSRP1/Dre4 for FACT), 1 × 10^6 S2 cells were washed in PBS with 2% BSA and then incubated in PBS containing 50 μg/ml propidium iodide, 200 μg/ml RNase A, and 0.1% Triton X-100 for 15 min at 25°C in the dark. Samples were analyzed on a BD FACSCaliber Flow Cytometer and analyzed using FloJo.

Imaging

All images were taken at 25°C on an Olympus Fluorescence Microscope (PersonalDV; Applied Precision) equipped with a 60× 1.42 NA or a 100× 1.40 NA oil-immersion objective (Olympus) and a CoolSnap HQ_2 Camera (Photometrics), keeping exposure conditions constant between all samples. Images were acquired and deconvolved using softWoRx (Applied Precision), maintaining the scaling constant between samples, and all images were saved as Photoshop files. Figures were assembled in Adobe Illustrator. See the Supplemental Experimental Procedures for image quantifications.

Chromatin Immunoprecipitation

ChIP was performed using the MAGnify Kit (Life Technologies). 10^6 cells (~10 μg DNA) was used for each IP, and chromatin was sheared to fragments 100–300 bp long. 1 μl of anti-CENP-A (rabbit, Active Motif), anti-SSRP1 (Nakayama et al., 2007), anti-GFP (Abcam), or anti-RNAPIIS2p (Abcam) were coupled to 10 μl beads for 2 hr and mixed with chromatin overnight at 4°C. Immunoprecipitated DNA was eluted in 50 μl of elution buffer and analyzed by qPCR. Normalization was performed using the following formula: 100 × $AE^{(averageCT\ INPUT\ -\ averageCT\ IP)}$, where AE is the amplification efficiency calculated by the formula AE = $10^{(-1/slope)}$. The values obtained for induced cells were normalized by those for uninduced cells to calculate enrichment. For ChIP-seq, DNA from three independent ChIP experiments were pooled and made into libraries with the TruSeq ChIP Kit (Illumina). Samples were run on a MiSeq using the Reagent Kit (v. 3). See the Supplemental Experimental Procedures for mapping information.

Statistical Methods

SE, SD, and CI were calculated using Numbers (Apple). Unpaired t test and chi-square tests were performed in Prism (GraphPad). See the Supplemental Experimental Procedures for statistical analysis of next-generation sequencing data.

ACCESSION NUMBERS

The accession number for the ChIP-seq and RNA-seq raw data reported in this paper is NCBI: SRP059507.

SUPPLEMENTAL INFORMATION

Supplemental Information includes Supplemental Experimental Procedures, five figures, and two tables and can be found with this article online at http://dx.doi.org/10.1016/j.devcel.2015.05.012.

ACKNOWLEDGMENTS

We thank Bo Reese (CGI) for sequencing support, G. Karpen, S. Hirose, A. Straight, and P. Heun for reagents, I. Cheeseman for critically reading the manuscript, L. Core for suggestions and help with ChIP-chip data analysis, and the Drosophila RNAi Screening Center (DRSC) for resources. This work was supported by awards from the NSF (1024973) (to B.G.M.) and the NIH (GM108829) (to B.G.M.). D.M.G. is supported by grants from Cancer Research UK (C3/A11431) and the Medical Research Council (G1001696); Z.L. is supported by a long-term FEBS Fellowship; and R.J.O. is supported by an NSF award (1244146).

Received: October 7, 2014
Revised: April 9, 2015
Accepted: May 18, 2015
Published: July 6, 2015

REFERENCES

Adolph, S., Brüsselbach, S., and Müller, R. (1993). Inhibition of transcription blocks cell cycle progression of NIH3T3 fibroblasts specifically in G1. J. Cell Sci. *105*, 113–122.

Barnhart, M.C., Kuich, P.H., Stellfox, M.E., Ward, J.A., Bassett, E.A., Black, B.E., and Foltz, D.R. (2011). HJURP is a CENP-A chromatin assembly factor sufficient to form a functional de novo kinetochore. J. Cell Biol. *194*, 229–243.

Belotserkovskaya, R., Oh, S., Bondarenko, V.A., Orphanides, G., Studitsky, V.M., and Reinberg, D. (2003). FACT facilitates transcription-dependent nucleosome alteration. Science *301*, 1090–1093.

Bernad, R., Sánchez, P., Rivera, T., Rodríguez-Corsino, M., Boyarchuk, E., Vassias, I., Ray-Gallet, D., Arnaoutov, A., Dasso, M., Almouzni, G., and Losada, A. (2011). Xenopus HJURP and condensin II are required for CENP-A assembly. J. Cell Biol. *192*, 569–582.

Birch, J.L., Tan, B.C., Panov, K.I., Panova, T.B., Andersen, J.S., Owen-Hughes, T.A., Russell, J., Lee, S.C., and Zomerdijk, J.C. (2009). FACT facilitates chromatin transcription by RNA polymerases I and III. EMBO J. *28*, 854–865.

Blower, M.D., and Karpen, G.H. (2001). The role of Drosophila CID in kinetochore formation, cell-cycle progression and heterochromatin interactions. Nat. Cell Biol. *3*, 730–739.

Blower, M.D., Sullivan, B.A., and Karpen, G.H. (2002). Conserved organization of centromeric chromatin in flies and humans. Dev. Cell *2*, 319–330.

Bodor, D.L., Valente, L.P., Mata, J.F., Black, B.E., and Jansen, L.E. (2013). Assembly in G1 phase and long-term stability are unique intrinsic features of CENP-A nucleosomes. Mol. Biol. Cell *24*, 923–932.

Bunch, T.A., Grinblat, Y., and Goldstein, L.S. (1988). Characterization and use of the Drosophila metallothionein promoter in cultured Drosophila melanogaster cells. Nucleic Acids Res. *16*, 1043–1061.

Camahort, R., Li, B., Florens, L., Swanson, S.K., Washburn, M.P., and Gerton, J.L. (2007). Scm3 is essential to recruit the histone h3 variant cse4 to centromeres and to maintain a functional kinetochore. Mol. Cell *26*, 853–865.

Carone, D.M., Longo, M.S., Ferreri, G.C., Hall, L., Harris, M., Shook, N., Bulazel, K.V., Carone, B.R., Obergfell, C., O'Neill, M.J., and O'Neill, R.J. (2009). A new class of retroviral and satellite encoded small RNAs emanates from mammalian centromeres. Chromosoma *118*, 113–125.

Carone, D.M., Zhang, C., Hall, L.E., Obergfell, C., Carone, B.R., O'Neill, M.J., and O'Neill, R.J. (2013). Hypermorphic expression of centromeric retroelement-encoded small RNAs impairs CENP-A loading. Chromosome Res. *21*, 49–62.

Chan, F.L., and Wong, L.H. (2012). Transcription in the maintenance of centromere chromatin identity. Nucleic Acids Res. *40*, 11178–11188.

Chan, F.L., Marshall, O.J., Saffery, R., Kim, B.W., Earle, E., Choo, K.H., and Wong, L.H. (2012). Active transcription and essential role of RNA polymerase II at the centromere during mitosis. Proc. Natl. Acad. Sci. USA *109*, 1979–1984.

Chen, C.C., Greene, E., Bowers, S.R., and Mellone, B.G. (2012). A role for the CAL1-partner Modulo in centromere integrity and accurate chromosome segregation in Drosophila. PLoS ONE *7*, e45094.

Chen, C.C., Dechassa, M.L., Bettini, E., Ledoux, M.B., Belisario, C., Heun, P., Luger, K., and Mellone, B.G. (2014). CAL1 is the Drosophila CENP-A assembly factor. J. Cell Biol. *204*, 313–329.

Choi, E.S., Strålfors, A., Castillo, A.G., Durand-Dubief, M., Ekwall, K., and Allshire, R.C. (2011). Identification of noncoding transcripts from within CENP-A chromatin at fission yeast centromeres. J. Biol. Chem. *286*, 23600–23607.

De Rop, V., Padeganeh, A., and Maddox, P.S. (2012). CENP-A: the key player behind centromere identity, propagation, and kinetochore assembly. Chromosoma *121*, 527–538.

Deyter, G.M., and Biggins, S. (2014). The FACT complex interacts with the E3 ubiquitin ligase Psh1 to prevent ectopic localization of CENP-A. Genes Dev. *28*, 1815–1826.

Dunleavy, E.M., Roche, D., Tagami, H., Lacoste, N., Ray-Gallet, D., Nakamura, Y., Daigo, Y., Nakatani, Y., and Almouzni-Pettinotti, G. (2009). HJURP is a cell-cycle-dependent maintenance and deposition factor of CENP-A at centromeres. Cell *137*, 485–497.

Dunleavy, E.M., Almouzni, G., and Karpen, G.H. (2011). H3.3 is deposited at centromeres in S phase as a placeholder for newly assembled CENP-A in G_1 phase. Nucleus *2*, 146–157.

Erhardt, S., Mellone, B.G., Betts, C.M., Zhang, W., Karpen, G.H., and Straight, A.F. (2008). Genome-wide analysis reveals a cell cycle-dependent mechanism controlling centromere propagation. J. Cell Biol. *183*, 805–818.

Foltz, D.R., Jansen, L.E., Black, B.E., Bailey, A.O., Yates, J.R., 3rd, and Cleveland, D.W. (2006). The human CENP-A centromeric nucleosome-associated complex. Nat. Cell Biol. *8*, 458–469.

Foltz, D.R., Jansen, L.E., Bailey, A.O., Yates, J.R., 3rd, Bassett, E.A., Wood, S., Black, B.E., and Cleveland, D.W. (2009). Centromere-specific assembly of CENP-a nucleosomes is mediated by HJURP. Cell *137*, 472–484.

Hemmerich, P., Weidtkamp-Peters, S., Hoischen, C., Schmiedeberg, L., Erliandri, I., and Diekmann, S. (2008). Dynamics of inner kinetochore assembly and maintenance in living cells. J. Cell Biol. *180*, 1101–1114.

Hondele, M., and Ladurner, A.G. (2013). Catch me if you can: how the histone chaperone FACT capitalizes on nucleosome breathing. Nucleus *4*, 443–449.

Hondele, M., Stuwe, T., Hassler, M., Halbach, F., Bowman, A., Zhang, E.T., Nijmeijer, B., Kotthoff, C., Rybin, V., Amlacher, S., et al. (2013). Structural basis of histone H2A-H2B recognition by the essential chaperone FACT. Nature *499*, 111–114.

Jacob, F., and Monod, J. (1961). Genetic regulatory mechanisms in the synthesis of proteins. J. Mol. Biol. *3*, 318–356.

Jansen, L.E., Black, B.E., Foltz, D.R., and Cleveland, D.W. (2007). Propagation of centromeric chromatin requires exit from mitosis. J. Cell Biol. *176*, 795–805.

Kharchenko, P.V., Alekseyenko, A.A., Schwartz, Y.B., Minoda, A., Riddle, N.C., Ernst, J., Sabo, P.J., Larschan, E., Gorchakov, A.A., Gu, T., et al. (2011). Comprehensive analysis of the chromatin landscape in Drosophila melanogaster. Nature *471*, 480–485.

Krogan, N.J., Kim, M., Ahn, S.H., Zhong, G., Kobor, M.S., Cagney, G., Emili, A., Shilatifard, A., Buratowski, S., and Greenblatt, J.F. (2002). RNA polymerase II elongation factors of Saccharomyces cerevisiae: a targeted proteomics approach. Mol. Cell. Biol. *22*, 6979–6992.

LeRoy, G., Orphanides, G., Lane, W.S., and Reinberg, D. (1998). Requirement of RSF and FACT for transcription of chromatin templates in vitro. Science *282*, 1900–1904.

Marshall, O.J., Chueh, A.C., Wong, L.H., and Choo, K.H. (2008). Neocentromeres: new insights into centromere structure, disease development, and karyotype evolution. Am. J. Hum. Genet. *82*, 261–282.

Mellone, B.G., Grive, K.J., Shteyn, V., Bowers, S.R., Oderberg, I., and Karpen, G.H. (2011). Assembly of Drosophila centromeric chromatin proteins during mitosis. PLoS Genet. *7*, e1002068.

Mendiburo, M.J., Padeken, J., Fülöp, S., Schepers, A., and Heun, P. (2011). Drosophila CENH3 is sufficient for centromere formation. Science *334*, 686–690.

Nakano, M., Cardinale, S., Noskov, V.N., Gassmann, R., Vagnarelli, P., Kandels-Lewis, S., Larionov, V., Earnshaw, W.C., and Masumoto, H. (2008). Inactivation of a human kinetochore by specific targeting of chromatin modifiers. Dev. Cell *14*, 507–522.

Nakayama, T., Nishioka, K., Dong, Y.X., Shimojima, T., and Hirose, S. (2007). Drosophila GAGA factor directs histone H3.3 replacement that prevents the heterochromatin spreading. Genes Dev. *21*, 552–561.

Ohkuni, K., and Kitagawa, K. (2011). Endogenous transcription at the centromere facilitates centromere activity in budding yeast. Curr. Biol. *21*, 1695–1703.

Okada, M., Okawa, K., Isobe, T., and Fukagawa, T. (2009). CENP-H-containing complex facilitates centromere deposition of CENP-A in cooperation with FACT and CHD1. Mol. Biol. Cell *20*, 3986–3995.

Orphanides, G., LeRoy, G., Chang, C.H., Luse, D.S., and Reinberg, D. (1998). FACT, a factor that facilitates transcript elongation through nucleosomes. Cell *92*, 105–116.

Orphanides, G., Wu, W.H., Lane, W.S., Hampsey, M., and Reinberg, D. (1999). The chromatin-specific transcription elongation factor FACT comprises human SPT16 and SSRP1 proteins. Nature *400*, 284–288.

Perpelescu, M., Nozaki, N., Obuse, C., Yang, H., and Yoda, K. (2009). Active establishment of centromeric CENP-A chromatin by RSF complex. J. Cell Biol. *185*, 397–407.

Pfaffl, M.W. (2001). A new mathematical model for relative quantification in real-time RT-PCR. Nucleic Acids Res. *29*, e45.

Phansalkar, R., Lapierre, P., and Mellone, B.G. (2012). Evolutionary insights into the role of the essential centromere protein CAL1 in Drosophila. Chromosome Res. *20*, 493–504.

Pidoux, A.L., Choi, E.S., Abbott, J.K., Liu, X., Kagansky, A., Castillo, A.G., Hamilton, G.L., Richardson, W., Rappsilber, J., He, X., and Allshire, R.C. (2009). Fission yeast Scm3: A CENP-A receptor required for integrity of subkinetochore chromatin. Mol. Cell *33*, 299–311.

Quénet, D., and Dalal, Y. (2014). A long non-coding RNA is required for targeting centromeric protein A to the human centromere. eLife *3*, e03254.

Rošić, S., Köhler, F., and Erhardt, S. (2014). Repetitive centromeric satellite RNA is essential for kinetochore formation and cell division. J. Cell Biol. *207*, 335–349.

Sanchez-Pulido, L., Pidoux, A.L., Ponting, C.P., and Allshire, R.C. (2009). Common ancestry of the CENP-A chaperones Scm3 and HJURP. Cell *137*, 1173–1174.

Saunders, A., Werner, J., Andrulis, E.D., Nakayama, T., Hirose, S., Reinberg, D., and Lis, J.T. (2003). Tracking FACT and the RNA polymerase II elongation complex through chromatin in vivo. Science *301*, 1094–1096.

Schuh, M., Lehner, C.F., and Heidmann, S. (2007). Incorporation of Drosophila CID/CENP-A and CENP-C into centromeres during early embryonic anaphase. Curr. Biol. *17*, 237–243.

Schwartz, B.E., and Ahmad, K. (2005). Transcriptional activation triggers deposition and removal of the histone variant H3.3. Genes Dev. *19*, 804–814.

Shimojima, T., Okada, M., Nakayama, T., Ueda, H., Okawa, K., Iwamatsu, A., Handa, H., and Hirose, S. (2003). Drosophila FACT contributes to Hox gene expression through physical and functional interactions with GAGA factor. Genes Dev. *17*, 1605–1616.

Shuaib, M., Ouararhni, K., Dimitrov, S., and Hamiche, A. (2010). HJURP binds CENP-A via a highly conserved N-terminal domain and mediates its deposition at centromeres. Proc. Natl. Acad. Sci. USA *107*, 1349–1354.

Stoler, S., Rogers, K., Weitze, S., Morey, L., Fitzgerald-Hayes, M., and Baker, R.E. (2007). Scm3, an essential Saccharomyces cerevisiae centromere protein required for G2/M progression and Cse4 localization. Proc. Natl. Acad. Sci. USA *104*, 10571–10576.

Straight, A.F., Belmont, A.S., Robinett, C.C., and Murray, A.W. (1996). GFP tagging of budding yeast chromosomes reveals that protein-protein interactions can mediate sister chromatid cohesion. Curr. Biol. *6*, 1599–1608.

Sullivan, B.A. (2010). Optical mapping of protein-DNA complexes on chromatin fibers. Methods Mol. Biol. *659*, 99–115.

Topp, C.N., Zhong, C.X., and Dawe, R.K. (2004). Centromere-encoded RNAs are integral components of the maize kinetochore. Proc. Natl. Acad. Sci. USA *101*, 15986–15991.

Whitfield, M.L., Sherlock, G., Saldanha, A.J., Murray, J.I., Ball, C.A., Alexander, K.E., Matese, J.C., Perou, C.M., Hurt, M.M., Brown, P.O., and Botstein, D. (2002). Identification of genes periodically expressed in the human cell cycle and their expression in tumors. Mol. Biol. Cell *13*, 1977–2000.

Xin, H., Takahata, S., Blanksma, M., McCullough, L., Stillman, D.J., and Formosa, T. (2009). yFACT induces global accessibility of nucleosomal DNA without H2A-H2B displacement. Mol. Cell *35*, 365–376.

Developmental Cell

Supplemental Information

Establishment of Centromeric Chromatin by the CENP-A Assembly Factor CAL1 Requires FACT-Mediated Transcription

Chin-Chi Chen, Sarion Bowers, Zoltan Lipinszki, Jason Palladino, Sarah Trusiak, Emily Bettini, Leah Rosin, Marcin R. Przewloka, David M. Glover, Rachel J. O'Neill , and Barbara G. Mellone

Supplemental Information

Inventory of supplementary material

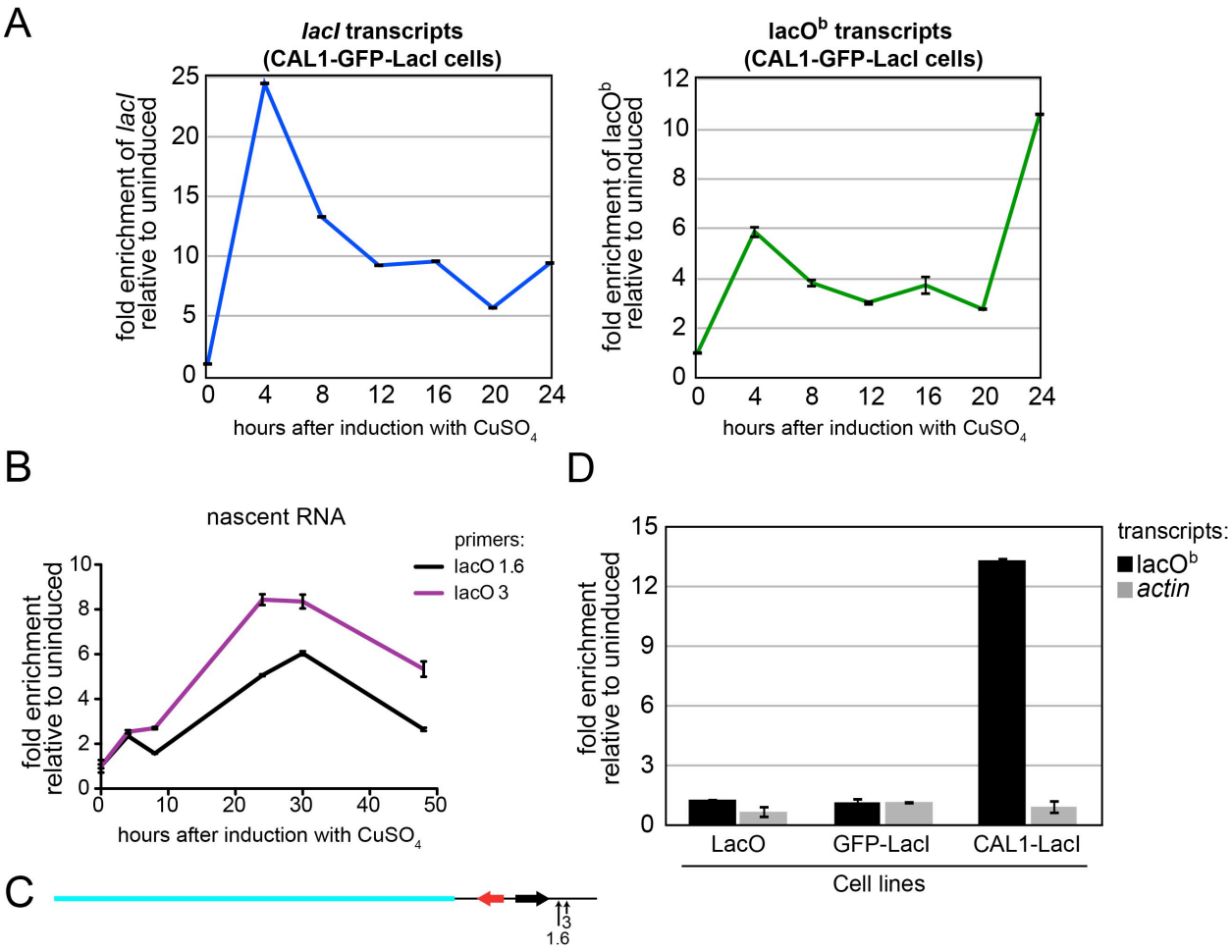

Figure S1, related to Figure 1. The transcription of lacO^b is continuous and correlates specifically with CENP-A assembly.

A) qRT-PCR analysis of CAL1-GFP-LacI transcripts (left, blue) and lacO^b (right, green) in induced CAL1-GFP-LacI cells at the indicated times. Error bars, SD of 3 technical replicates. B) qRT-PCR analysis of nascent lacO^b transcripts in a time course (0, 4, 8, 24, 30, 48h) after induction with $CuSO_4$ using two primer sets, 1.6 (black) and 3 (purple). Error bars, SD of 3 technical replicates. C) lacO diagram showing position of primer sets 1.6 and 3. D) Transcription of lacO^b (primer 1.6) and *actin* (RNAPII control gene), relative to uninduced, determined by qRT-PCR in the indicated cell lines after 24h induction with $CuSO_4$. Error bars show the 95% CI of 3 technical replicates.

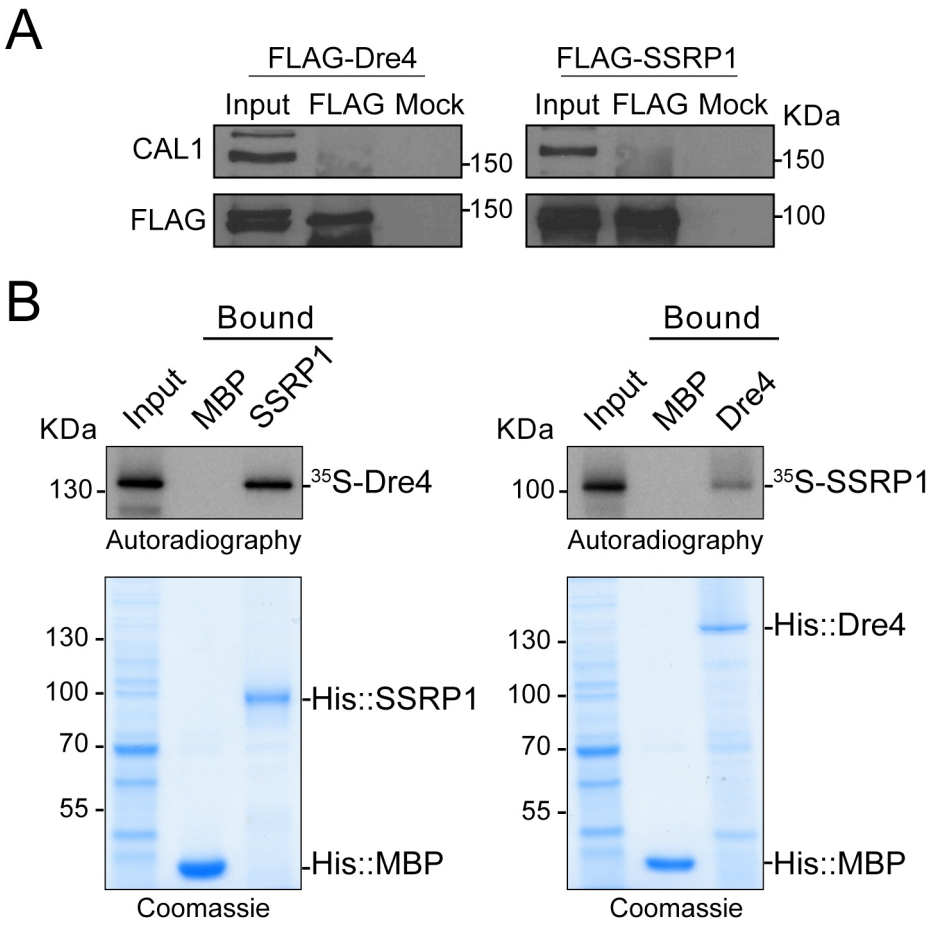

Figure S2, related to Figure 3. Interactions between FACT subunits and CAL1

A) Western blot with anti-CAL1 (top) or anti-FLAG (bottom) on input and IP performed with anti-FLAG coupled beads (FLAG) or beads alone (mock) from total nuclear extracts. Cell lines were stable S2 expressing either FLAG-Dre4 or FLAG-SSRP1. B) Direct interaction between SSRP1 and Dre4 was examined *in vitro* by incubating ^{35}S-methionine-labeled Dre4 (produced by IVTT) with recombinant His::SSRP1 (left panel) or ^{35}S-methionine-labeled SSRP1 with His::Dre4 (right panel) bound to Ni-NTA beads. His::MBP (MBP) on Ni-NTA beads was used as a negative control.

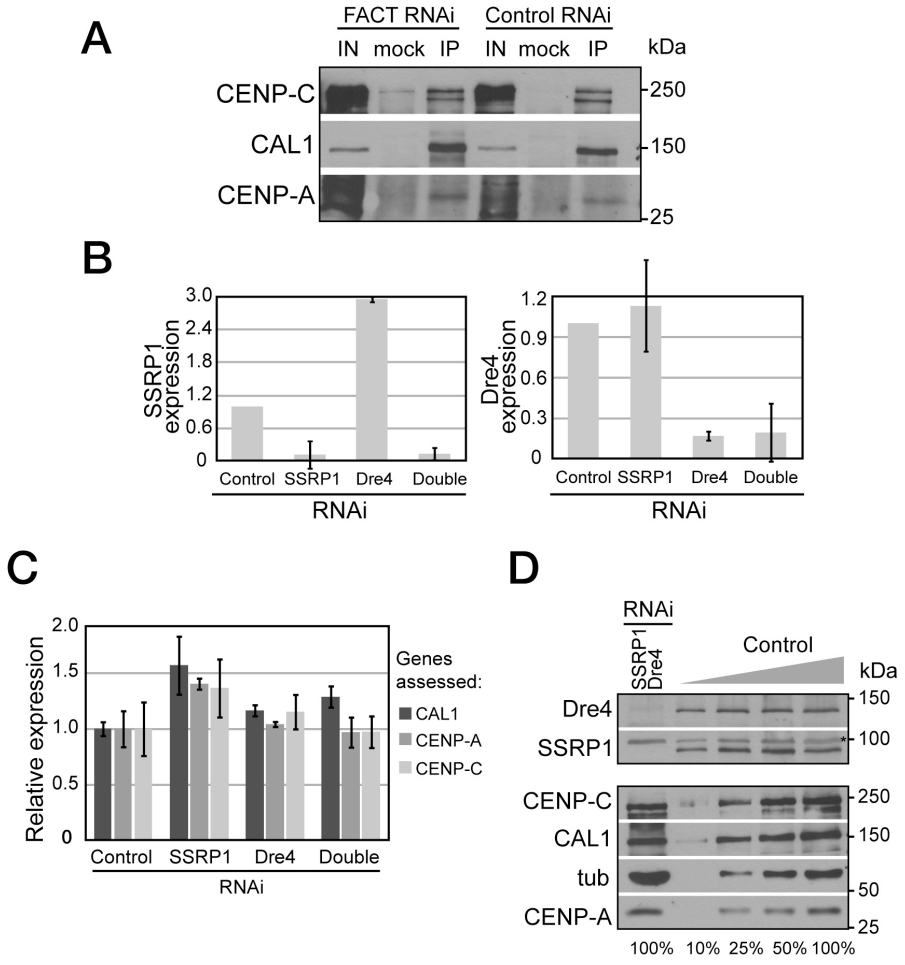

Figure S3, related to Figure 5. CAL1, CENP-A and CENP-C mRNA and protein levels, and their reciprocal association are unaffected by FACT RNAi

A) CAL1 IPs from cells in which FACT was depleted by RNAi. Western blot was performed with the indicated antibodies on total nuclear extracts (IN) and material immunoprecipitated with anti CAL1 antibodies (IP) eluted from beads from control cells and cells where Dre4 and SSRP1 were knocked-down by RNAi. The control lane (mock) shows IPs in which the antibody was omitted. B) qRT-PCR assessing the expression levels of SSRP1 (left) and Dre4 (right) after 6 days RNAi of each gene singly and together (double). Values are normalized to the Bw RNAi (control). Error bars show the 95% CI of 3 technical replicates. C) qRT-PCR with *cal1, cenp-a* and *Cenp-c* primers showing the relative expression of these genes in the indicated RNAi conditions. Error bars show the 95% CI of 3 technical replicates. D) Semi-quantitative Western blot with the indicated antibodies of total protein extracts from control RNAi and Dre4 and SSRP1 double RNAi in S2 cells. The percent of extract loaded on a 10% SDS-PAGE are shown at the bottom of the blot.* Indicates a non-specific band.

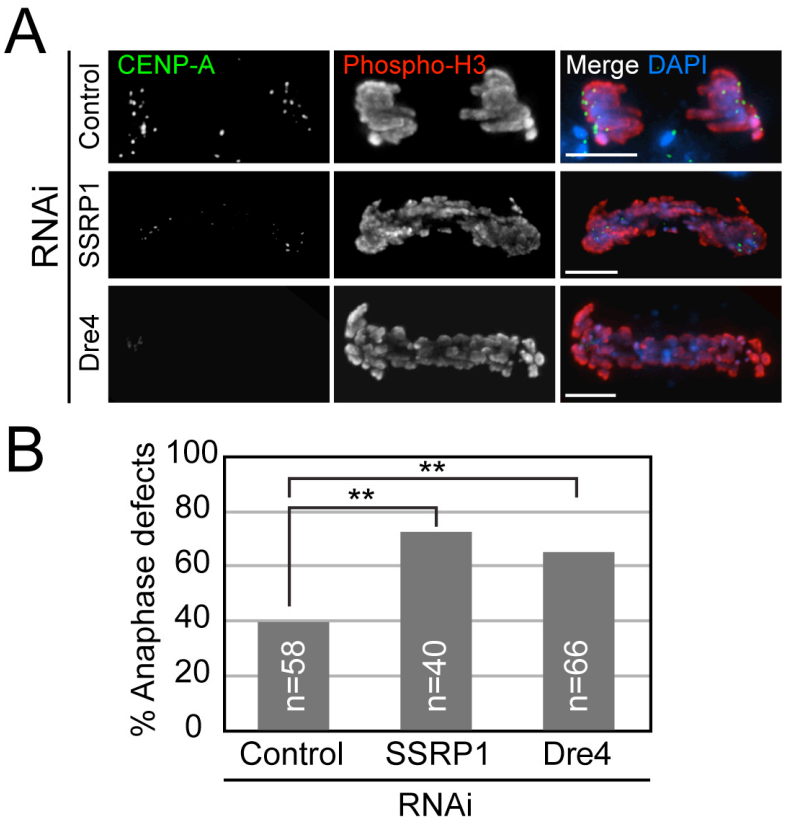

Figure S4, related to Figure 6. FACT RNAi leads to chromosome segregation defects in mitosis

A) Mitotic figures from S2 cells treated with control (Bw), SSRP1, and Dre4 RNAi. CENP-A is shown in green, phosphorylated H3-Ser10 is shown in red. Bar 5μm. B) Quantification of the frequency of chromosome missegregation in mitosis for the cells shown in A. ** $p<0.005$ (unpaired t-test). Note that SSRP1 was previously reported to affect spindle structure (Zeng et al., 2010).

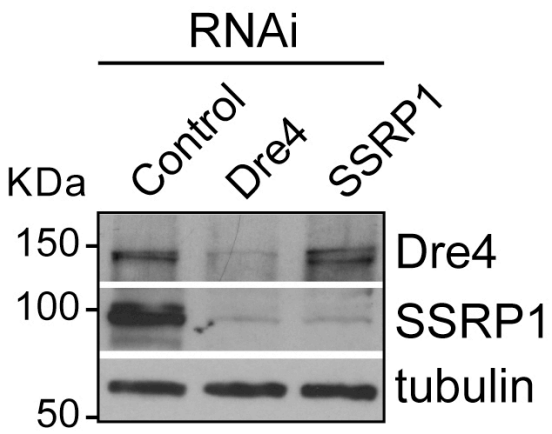

Figure S5, related to Figure 7. RNAi of Dre4 causes a reduction in SSRP1 protein levels

A) Western blot with the indicated antibodies of total protein extracts from S2 cells treated with control, Dre4, and SSRP1 RNAi. In Dre4 RNAi, SSRP1 protein levels decrease, suggesting that it becomes unstable in the absence of Dre4.

Supplementary Tables

Table S1, related to Figure 3. Summary of CAL1-FLAG mass spectrometry results

MASCOT score and % coverage are shown for the CAL1 interactors that were confirmed by IP (this work and (Chen et al., 2012)). Note that our chromatin-associated large-scale IP was less successful than the chromatin-free IP. n/a= not applicable.

	MASCOT		% Coverage	
	Chromatin Free	Chromatin Associated	Chromatin Free	Chromatin Associated
Dre4/Spt16	1099	390	47.4	21.7
SSRP1	n/a	136	n/a	16.3
CAL1 (bait)	221	n/a	19.7	n/a
CENP-A/CID	32	n/a	32	n/a
Modulo	177	n/a	33.4	n/a

Table S2, related to Figure 5. Effect of FACT RNAi on the expression of 8 genes associated with Dre4

qRT-PCR data using the indicated primer pairs (obtained from the DRSC database) and *Rp49* as a reference gene for 8 hand-picked RNAPII transcribed genes that are expressed at low, moderate, and high levels in S2 cells (as reported by modENCODE) and that are associated with Dre4/Spt16 by ChIP-chip (Kharchenko et al., 2011). Transcript levels for FACT RNAi (carried out by simultaneous RNAi for Dre4 and SSRP1) were normalized by the control. Shown are the means of three experiments ± SD. Most genes were unchanged or slightly more expressed upon FACT RNAi.

Gene	Expression level reported for S2 cells	Expression change in FACT RNAi relative to control	Primer set used (DRSC)
Rpl5	high	1.24 ± 0.06	PP16712
Ef2b	high	1.74 ± 0.02	PP35106
Pdcd4	moderate	1.92 ± 0.06	PP1031
CG9934	moderate	2.32 ± 0.07	PP6054
CG7970	moderate	1.54 ± 0.1	PP10328
Esyt2	low	4.18 ± 2.24	PP27131
Dyb	low	2.10 ± 0.18	PP24370
CG8399	low	1.23 ± 0.21	PP34732

Supplementary Experimental Procedures

Large-scale immunoprecipitations and mass spectrometry

FLAG-CAL1 complexes were isolated and purified from chromatin-free extracts generated from $2x10^6$ S2 cells, as described previously (Chen et al., 2012; Mellone et al., 2011). FLAG-CAL1 complexes from chromatin-associated complexes were generated by homogenization in 5ml ice-cold Buffer A (20mM HEPES pH 7.4; 10mM KCl; 1.5mM $MgCl_2$; 0.34M Sucrose; 0.2% Triton-X 100; 10% Glycerol; 1mM DTT), with protease inhibitors (Roche) and 1mM PMSF, followed by consecutive extractions in buffer B (Buffer A with 150mM KCl, protease inhibitor cocktail and 1mM PMSF), buffer C (0.34M Sucrose 50mM Tris pH 7.4; 1.5mM NaCl; 5mM $MgCl_2$; 1mM EGTA; 0.04% Triton-X 100; 1mM DTT, protease inhibitors and 1mM PMSF) and buffer D (10mM HEPES pH7.4; 2mM $MgCl_2$; 250mM Sucrose). 800µl of Buffer E (10mM HEPES pH 7.4; 2mM $MgCl_2$; 0.5M Sucrose) was pipetted underneath the suspension and centrifuged at 500 g for 5 min. The pellet was resuspended in 400µl Buffer F (2mM EGTA; 1mM DTT; protease inhibitor cocktail), followed by resuspension in digestion Buffer (10mM Tris pH 7.4; 150mM NaCl; 1mM $MgCl_2$; 0.025% NP-40; protease inhibitor cocktail; 1mM PMSF; 4µl Benzonase) for 1 h at 4°C. After stopping the digestion with EDTA, the extract was added to 100µl M2-FLAG agarose beads (Sigma). After washing, complexes were eluted with 400mM FLAG peptide (Sigma-Aldrich). The eluted FLAG-CAL1 complex was reduced, carboxamidomethylated, digested with trypsin and LysC and subjected to LC-MS/MS on a Waters/Micromass AB QSTAR Elite mass spectrometer (Keck Biotechnology Resource, Yale School of Medicine). MS/MS spectra were analyzed using MASCOT (Matrix Science).

Cell culture and treatments

Cells were cultured at 25°C in Schneider medium as described (Chen et al., 2014) with addition of 150µg/ml hygromycin and/or 2 µg/ml puromycin if stably transfected. Stable S2 cells containing an integrated lacO array (pAFS52; (Straight et al., 1996)) were described before (Chen et al., 2014; Mendiburo et al., 2011). Note that this line is polyclonal and approx. 65% of cells bears the lacO insertion and the CAL1-GFP-LacI transgenes. Additional stable S2 cells were generated by transfection of $1x10^6$ cells with 2µg of plasmid DNA, alongside 2µg of the pHygro plasmid using cellfectin (Invitrogen). Cells were grown for 3 days before addition of 450µg/ml hygromycin to select for transfected cells. Transfection efficiency was determined by IF and Western blotting with the appropriate antibodies. Stable S2 cells harboring the lacO array were re-thawed after one month in culture to prevent shrinking and loss of the lacO array.

Transient transfections were performed using FuGENE HD (Promega) with 2µg of plasmid DNA (pMT-CAL1-GFP-LacI; pAS52-lacO; pMT-CAL1Δ1-40 -GFP-LacI), incubated for 2 days, and induced with 0.5mM $CuSO_4$ for 24h.

Induction of CAL1-GFP-LacI or GFP-LacI was performed by addition of 0.5mM $CuSO_4$ to the growth medium and incubation at 25°C for 1-48h. Uninduced samples followed the same treatments as the induced without the addition of $CuSO_4$.

RNAi

Double-stranded RNAs (dsRNA) against *dre4, ssrp1, cal1,* and *brown* (negative control) were generated using the Ambion T7 Synthesis kit, using primers obtained from the DGRC (see Supplementary experimental procedures, primers).

RNAi was performed using 10µg of dsRNA transfected into $1x10^6$ S2 cells using DOTAP (Roche). Cells were either incubated for four days after which $1x10^6$ cells were re-transfected with 10µg of dsRNA and incubated for a further 2 days (Figure 6E-F), or were incubated for 6 days after a single transfection (Figure 6A-D). Depletion of FACT by Western blot occurred 4 days after RNAi, while complete loss of endogenous CENP-A IF signal occurred after double RNAi treatment for 6 a total of days.

To visualize H3.1 and H3.3 occupancy we performed FACT depletion by RNAi for 72h before transient transfection with either pMT-H3.1-V5 or pMT-H3.3-V5 using FUGENE (Promega). Cells were incubated for an additional 48h after which they were induced for 24h with 100µM $CuSO_4$. Cells were then processed for fiber IF; transfection efficiency and successful depletion of Dre4 and SSRP1 was confirmed by Western blotting.

Image quantification

For the quench-chase-pulse, we used manual quantification to determine signal intensity of TMR-CENP-A foci within the cell nucleus. Intensity was categorized as follows: strong signal = >800 (A.U.); medium signal = 200-800; weak/no signal = <200. 100 cells per replicate experiment were scored, three replicates were performed.

For the CENP-A IF signal we used Softworx Suite's 2D Polygon Finder function. The total intensity/per cell was averaged for 50-100 cells from each condition. The resulting averages for each condition were averaged again across three independent replicates.

CENP-A fibers were measured using the Measure Distance tool in Softworx Suite by placing one point at each end of the CENP-A signal on a single continuous fiber (defined by the presence of CENP-A signal at least 1/3 of the max intensity for that stretch).

DNA constructs

The lacO plasmid was described previously (Straight et al., 1996). *dre4* and *ssrp1* were cloned into pCopia-FLAG vector by PCR (see 'primers used in this study' section below) from cDNA clones obtained from the DGRC adding AscI/PacI restriction sites. For the *in vitro* binding assays, the coding sequences (*dre4 and ssrp1*) were inserted into pDONR221 using the Gateway System (Life Technologies) or PCR amplified to include a T7 promoter, a Kozak sequence, a start codon and 4 stop codons in the case of CAL1Δ1-40. Expression clones were then made using pDEST17. pMT-H3.1-V5 and pMT-H3.3-V5 were generated by topo-cloning PCR products amplified from genomic DNA using the DES TOPO TA Expression Kit (Invitrogen). All plasmids were verified by sequencing.

Protein expression and affinity purification

The expression of His-tagged Dre4, SSRP1 and MBP was induced in *E. coli* strain Rosetta 2(DE3)pLysS Single (Novagen) with 0.2mM IPTG at 22°C for 5h. Cells were lysed by sonication in extraction buffer containing 20mM Tris pH 8.0, 500mM NaCl, 20mM imidazole and 5mM β-mercaptoethanol supplemented with 6M Guanidine hydrochloride. Recombinant proteins were immobilized onto Ni-NTA agarose beads under denaturing conditions according to the manufacturer (Qiagen). Refolding was performed using standard procedures: beads were gradually washed in extraction buffer supplemented with 0.1% Triton X-100 and 6 to 0M urea, respectively.

For the *in vitro* binding assay ^{35}S-methionine-labelled Dre4, SSRP1 or CAL1 (from pDEST24 or PCR product for CAL1Δ1-40) were expressed *in vitro* using the TNT T7 Quick Coupled Transcription/Translation System (IVTT) according to the manufacturer (Promega, L1170). After 2h incubation at 30°C IVTT reactions were treated with 10 Kunitz units DNase I (Sigma, D4263) for further 15 min to eliminate DNA, centrifuged at room temperature (21000 g, 5 min) and supernatants were directly used in *in vitro* binding assay.

SDS-PAGE and autoradiography for *in vitro* interaction assays

Protein samples (2-6% input and 30-50% bound proteins) were separated by 8% or 9% SDS-PAGE, gels were rinsed in water and stained with Bio-Safe Coomassie (Bio-Rad), scanned, dried on Whatman 3MM filter paper and directly used for autoradiography. Exposure to hypersensitive film (Kodak BioMax MS film) was performed at -80°C.

Detection of nascent RNA

Nascent RNA was isolated using the Click-iT nascent RNA capture kit (Life Technologies). Cells were either not induced (0h) or induced with 0.5mM $CuSO_4$ for 4, 8, 24, 30 and 48h and nascent RNA was labeled with EU for the last 4h of each time point (in the case of the uninduced 0h, no $CuSO_4$ was added and EU was added for 4h). Total RNA was isolated using the TRI-reagent (Sigma) and 5µg of total RNA were subjected to biotinylation followed by EU-labeled RNA purification using 40µl of streptavidin magnetic beads. The isolated RNAs were used as templates to synthesize cDNA using the iScript cDNA synthesis kit (Bio-Rad) and followed by qPCR.

ChIP-Seq and RNA-Seq mapping

Prior to mapping, all libraries were Illumina adaptor trimmed and filtered for quality scores 30 and greater using Trimmomatic version 0.32 (Bolger et al., 2014). Paired-end global alignments to the full LacO array and vector reference were performed using Bowtie2 version 2.2.2 (Langmead and Salzberg, 2012) under the --very-sensitive settings and allowing for an inter-mate distance of 100 to 300nt in the ChIP pools and 100 to 400nt for the RNA pools. Alignment files were filtered to report only read pairs that mapped concordantly with a mapping quality greater than 0.

To generate signal tracks for the ChIP-Seq, peak-calling was performed on each of the lacO mapped pools using MACS2 (Zhang et al., 2008) with the recommended broad peak-calling parameters, --no-model and --no-lambda. The coverage values in the bedgraph output files were converted to fragments per million reads to normalize coverage to the sequencing depth of each library. Signal tracks were visualized using IGV (Robinson et al., 2011). In addition, MACS2 was used to compute the fold enrichment of called peaks, and corresponding p- and q-values, for each induced pool over its corresponding uninduced control.

To calculate a p-value for differential expression in the RNA-Seq, the pools were aligned with TopHat to the LacO reference concatenated to the dm3 chromosome 2L and 3L reference sequences and processed through the Cufflinks suite (Trapnell et al., 2012). Default parameters were used, with the exception of an upper quartile normalization (-N) and multiple mapping read correction (-u). For the RNA-Seq data, a differential expression analysis was also performed to calculate the fragments per kilobase (FPKM) mapped for each pool. CAL1-GFP-LacI pool had an FPKM of 92.06, while the GFP-LacI pool had an FPKM of 45.88. This was found to be a differential expression to a p-value < 0.05%.

Co-immunoprecipitation of CAL1 and RNAPIIS2p

Chromatin associated extracts were isolated from $2x10^8$ S2 cells as described above and chromatin-containing pellets were digested either with 4µl of DNaseI (Promega) in digestion buffer (protease inhibitors,10 mM Tris-HCl, pH 7.4, 0.3 M NaCl, 1 mM $MgCl_2$, 0.025% NP-40) for 20 min at 37°C after which 2 mM EDTA was added to the extracts, or with $20U/10^8$ cells MNase (Zymo Research) in EX100 buffer (10 mM HEPES, pH 7.6; 100 mM NaCl; 1.5 mM $MgCl_2$; 2 mM $CaCl_2$;0.5 mM EGTA; 10% v/v glycerol; protease inhibitors) for 20 min at 26°C followed by termination with 10mM EGTA. The NaCl concentration was increased to 300 mM and the chromatin was centrifuged at 12,000g for 10 min at 4°C. The supernatant was then used as the input in the IPs. For IPs, 4µg of anti-CAL1 antibody (rabbit) or PBS (mock) was coupled to 25µl of Dynabeads Protein-A (Invitrogen) beads, following the manufacturer's instructions. The input was incubated with beads for 2h with rotation at 4°C. After three washes in cold PBS, bound proteins were eluted with 20µl of Laemmli buffer (100 mM Tris, pH 6.8; 4% SDS; 20% glycerol; 0.1% bromophenol blue; 300 mM 2-mercaptoethanol) and boiled 5 min at 95°C. 1.6% of the total input and 50% of the total IP were subjected to Western blot.

Primers used in this study

RNAi	
Dre4 R	TAATACGACTCACTATAGGGCAGCGACGAGGAAGATGTG
Dre4 S	TAATACGACTCACTATAGGGCTGACAAATGTGGCCTCTGG
SSRP1 R	TAATACGACTCACTATAGGGCGAAAATCCGGGCATAAAGGT
SSRP1 S	TAATACGACTCACTATAGGGCTTGCTCTTCTTCTTGGCAGG
Bw R	TAATACGACTCACTATAGGGCGATATTATCGATGTCGATCCAG
Bw S	TAATACGACTCACTATAGGGCCTATGGCGTGACGTATATATTT
CAL1 R	TAATACGACTCACTATAGGGCTGGATGCCAGGAAAGTTAGT
CAL1 S	TAATACGACTCACTATAGGGCCTATAGGGATTGTTGATATCAGC
Cloning	
SSRP1 F (flag)	CAGTGGCGCGCCATGACAGACTCTCTGGAG
SSRP1 R (flag)	CAGTTTAATTAACTAATCACTGGCCTCATCTTCC
Dre4 F (flag)	CAGTACTAGTATGTCGAGCTTTGTGCTGG
Dre4 R (flag)	CATGGCGGCCGCCTAATGTCGCGACTTCTTCG
Dre4-GW-F	GGGGACAAGTTTGTACAAAAAAGCAGGCTTAATGTCGAGCTTTGTG CTGGACAAGG

Dre4-GW-R	GGGGACCACTTTGTACAAGAAAGCTGGGTACTAATGTCGCGACTTC TTCGACTTG
SSRP1-GW-F	GGGGACAAGTTTGTACAAAAAAGCAGGCTTAATGACAGACTCTCTG GAGTACAACG
SSRP1-GW-R	GGGGACCACTTTGTACAAGAAAGCTGGGTACTAATCACTGGCCTCA TCTTCCTCA
Cal1-GW-F	GGGGACAAGTTTGTACAAAAAAGCAGGCTTAATGGCGAATGCGGTG GTGGACGAGG
Cal1-GW-R	GGGGACCACTTTGTACAAGAAAGCTGGGTATTACTTGTCACCGGAA TTATTCTCG
qPCR	
Dre4 F	CCTGAAGCAGACGCAGAACATC
Dre4 R	CAAACGCTTGCCCTTCTTCGAG
SSRP1 F	AACGACATAAACGCCGAAGTGC
SSRP1 R	CCTTGCCGGTCTTGGTGTTC
CAL1 F	TGGTGGACGAGGAAACACTGG
CAL1 R	TCTATTTCCATGCCGTCTTCCAGG
CID F	TCTAGTGCGCGAGTTCATCGTG
CID R	AAGTACATCTCGCACGACTCCTG
CENP-C F	AGGGCGACCACGATCTACTC
CENP-C R	CCGTCCTTTGAAGATTTGCGTCG
Actin F	GATCTGTATGCCAACACCGT
Actin R	GCGGGGCAATGATCTTGATC
Rp49 F	CCGCTTCAAGGGACAGTATC
Rp49 R	GACAATCTCCTTGCGCTTCT
18S F	TGACGAAAAATAACAATACAGGACTCA
18S R	CAGACTTGCCCTCCAATT GG
lacO 1.6 F	CCCCGTAGAAAAGATCAAAGG
lacO 1.6 R	GCTGGTAGCGGTGGTTTTT
lacO 3 F	CGGATCAAGAGCTACCAACTC
lacO 3 R	CTTGAAGTGGTGGCCTAACT
LacI F	TATCCGCTGGATGACCAGGA
LacI R	CAGTCGCGTACCGTCTTCAT

In vitro transcription translation (IVTT)	
Cal1Δ1-40 F	GAATTAATACGACTCACTATAGGGAGAGCCGCCACCATGGCCGAGT TCGACAACTTGTTCCA
Cal1Δ1-40 R	TCATTACTATCATTACTTGTCACCGGAATTATTCTCGA

Supplementary References

Bolger, A.M., Lohse, M., and Usadel, B. (2014). Trimmomatic: a flexible trimmer for Illumina sequence data. Bioinformatics 30, 2114-2120.

Chen, C.C., Greene, E., Bowers, S.R., and Mellone, B.G. (2012). A Role for the CAL1-Partner Modulo in Centromere Integrity and Accurate Chromosome Segregation in Drosophila. PLoS One 7, e45094.

Erhardt, S., Mellone, B.G., Betts, C.M., Zhang, W., Karpen, G.H., and Straight, A.F. (2008). Genome-wide analysis reveals a cell cycle-dependent mechanism controlling centromere propagation. J Cell Biol 183, 805-818.

Kharchenko, P.V., Alekseyenko, A.A., Schwartz, Y.B., Minoda, A., Riddle, N.C., Ernst, J., Sabo, P.J., Larschan, E., Gorchakov, A.A., Gu, T., et al. (2011). Comprehensive analysis of the chromatin landscape in Drosophila melanogaster. Nature 471, 480-485.

Langmead, B., and Salzberg, S.L. (2012). Fast gapped-read alignment with Bowtie 2. Nature methods 9, 357-359.

Mellone, B.G., Grive, K.J., Shteyn, V., Bowers, S.R., Oderberg, I., and Karpen, G.H. (2011). Assembly of Drosophila centromeric chromatin proteins during mitosis. PLoS Genet 7, e1002068.

Robinson, J.T., Thorvaldsdottir, H., Winckler, W., Guttman, M., Lander, E.S., Getz, G., and Mesirov, J.P. (2011). Integrative genomics viewer. Nat Biotechnol 29, 24-26.

Straight, A.F., Belmont, A.S., Robinett, C.C., and Murray, A.W. (1996). GFP tagging of budding yeast chromosomes reveals that protein-protein interactions can mediate sister chromatid cohesion. Curr Biol 6, 1599-1608.

Trapnell, C., Roberts, A., Goff, L., Pertea, G., Kim, D., Kelley, D.R., Pimentel, H., Salzberg, S.L., Rinn, J.L., and Pachter, L. (2012). Differential gene and transcript expression analysis of RNA-seq experiments with TopHat and Cufflinks. Nat Protoc 7, 562-578.

Zeng, S.X., Li, Y., Jin, Y., Zhang, Q., Keller, D.M., McQuaw, C.M., Barklis, E., Stone, S., Hoatlin, M., Zhao, Y., et al. (2010). Structure-specific recognition protein 1 facilitates microtubule growth and bundling required for mitosis. Mol Cell Biol 30, 935-947.

Zhang, Y., Liu, T., Meyer, C.A., Eeckhoute, J., Johnson, D.S., Bernstein, B.E., Nusbaum, C., Myers, R.M., Brown, M., Li, W., et al. (2008). Model-based analysis of ChIP-Seq (MACS). Genome Biol 9, R137.